ARMY RESEARCH LABORATORY

White Sands Missile Range 2007 Urban Study: Data Processing – Volume DP-3 (Airflow Qualitative Assessment)

by Gail Vaucher and Manuel Bustillos

ARL-TR-4441 **May 2008**

NOTICES

Disclaimers

The findings in this report are not to be construed as an official Department of the Army position unless so designated by other authorized documents.

Citation of manufacturer's or trade names does not constitute an official endorsement or approval of the use thereof.

Destroy this report when it is no longer needed. Do not return it to the originator.

Army Research Laboratory
White Sands Missile Range, NM 88002-5501

ARL-TR-4441 **May 2008**

White Sands Missile Range 2007 Urban Study: Data Processing – Volume DP-3 (Airflow Qualitative Assessment)

Gail Vaucher and Manuel Bustillos
Computational and Information Sciences Directorate, ARL

REPORT DOCUMENTATION PAGE

Form Approved
OMB No. 0704-0188

1. REPORT DATE *(DD-MM-YYYY)*	2. REPORT TYPE	3. DATES COVERED (From - To)
May 2008	Final	

4. TITLE AND SUBTITLE
White Sands Missile Range 2007 Urban Study: Data Processing – Volume DP-3 (Airflow Qualitative Assessment)

5a. CONTRACT NUMBER

5b. GRANT NUMBER

5c. PROGRAM ELEMENT NUMBER

6. AUTHOR(S)
Gail Vaucher and Manuel Bustillos

5d. PROJECT NUMBER

5e. TASK NUMBER

5f. WORK UNIT NUMBER

7. PERFORMING ORGANIZATION NAME(S) AND ADDRESS(ES)
U.S. Army Research Laboratory
Computational and Information Sciences Directorate
Battlefield Environment Division (ATTN: AMSRD ARL CI ED)
White Sands Missile Range, NM 88002-5501

8. PERFORMING ORGANIZATION REPORT NUMBER
ARL-TR-4441

9. SPONSORING/MONITORING AGENCY NAME(S) AND ADDRESS(ES)

10. SPONSOR/MONITOR'S ACRONYM(S)

11. SPONSOR/MONITOR'S REPORT NUMBER(S)

12. DISTRIBUTION/AVAILABILITY STATEMENT
Approved for public release; distribution is unlimited.

13. SUPPLEMENTARY NOTES

14. ABSTRACT
Urban toxic chemical releases pose a threat to the military and civilians. The *White Sands Missile Range (WSMR) Urban Studies* address two critical elements in diagnosing airborne hazard releases, namely, airflow (chemical distribution) and stability (chemical concentration). This document provides a qualitative assessment of seven airflow features targeted by the *WSMR 2007 Urban Study* (*W07US*). The *W07US* stability assessment is published separately. The features identified for verification and characterization include the Fetch Flow, Velocity Acceleration, Velocity Deficit, Cavity Flows, Canyon Flows, Leeside Corner Eddies, and Reattachment Zone. Feature definitions, frequency of occurrences/day, and field study statistics are presented. Case studies enrich the text with excellent examples of inter-feature attributes and the detailed temporal and spatial urban characteristics. Suggestions for future airflow analysis work are interwoven throughout the text. The conclusions and recommendations recap key findings and "next step" suggestions for the *W07US* airflow qualitative assessment.

15. SUBJECT TERMS
W07US, urban study, airflow, qualitative assessment, velocity acceleration/deficit, cavity flow, canyon flow, reattachment zone, leeside eddies

16. SECURITY CLASSIFICATION OF:			17. LIMITATION OF ABSTRACT	18. NUMBER OF PAGES	19a. NAME OF RESPONSIBLE PERSON
a. REPORT	b. ABSTRACT	c. THIS PAGE			Gail Vaucher
U	U	U	UU	84	19b. TELEPHONE NUMBER (*Include area code*) (575) 678-3237

Standard Form 298 (Rev. 8/98)
Prescribed by ANSI Std. Z39.18

Contents

List of Figures

List of Tables

Acknowledgments

The authors would like to acknowledge Mr. Robert Brice and Mr. Sean D'Arcy for their invaluable participation in the acquisition of the *White Sands Missile Range 2007 Urban Study* airflow data.

Executive Summary

The release of toxic chemicals in an urban area poses a threat to both military and civilians. The U.S. Army Research Laboratory (ARL) has been working toward enhancing their current urban atmospheric intelligence so that a tool for guiding personnel into least hazardous or "safe" zones can be developed. The *White Sands Missile Range (WSMR) Urban Studies* have been addressing two critical atmospheric constituents in diagnosing the hazardous release of airborne elements, namely, airflow (which addresses toxic chemical distribution) and atmospheric stability (which addresses the toxic chemical concentration). In this document, a brief history of the evolving *WSMR Urban Study* research sets the stage for the report's main topic: a qualitative assessment of the airflow features targeted by the *WSMR 2007 Urban Study* (*W07US*) data collection. The *W07US* stability qualitative assessment is being published in a separate ARL technical report.

The seven airflow features identified for verification and characterization during *W07US* included the Fetch Flow, Velocity Acceleration, Velocity Deficit, Cavity Flows, Canyon Flows, Leeside Corner Eddies or Vortices, and Reattachment Zone. Idealized definitions for each flow feature are described. The frequency of occurrences by day and an average for the entire field study period are tabulated and graphically presented for each feature. Noteworthy attributes and trends within the statistical summaries are discussed. Time series case studies showing excellent examples of inter-feature attributes and the detailed nature of the temporal and spatial characteristics within an urban environment enrich the discussion section. Suggestions for future work on each airflow feature are interwoven throughout the text. The conclusions and recommendations recapitulate the key findings and "next step" suggestions for the *W07US* airflow qualitative assessment.

.

INTENTIONALLY LEFT BLANK.

1. Introduction

The destruction of the World Trade Center Twin Towers on 2001 September 11 raised the civilian concern for terrorist activities in an urban environment. On 2007 February 22, the release of toxic chemicals in the southwestern Bayaa neighborhood of Baghdad, Iraq, reinforced the need for atmospheric intelligence concerning the airflow and stability around occupied urban buildings. In this latter instance, 6 people were killed and more than 70 persons were hospitalized with respiratory problems (CNN, 2007).

The release of toxic chemicals in an urban area poses a threat to both military and civilians. The U.S. Army Research Laboratory (ARL) has been working toward enhancing their current urban atmospheric intelligence so that a tool for guiding personnel into least hazardous or "safe" zones can be developed. The *White Sands Missile Range (WSMR) Urban Studies* have been addressing two critical atmospheric constituents in diagnosing the hazardous release of airborne elements, namely, airflow (which addresses toxic chemical distribution) and atmospheric stability (which addresses the toxic chemical concentration).

The following report begins with a general overview of the *WSMR Urban Study* project and a description of the latest field study, *WSMR 2007 Urban Study* (*W07US*). An explanation of the post-*W07US* field study data processing plan and method introduces the primary topic of this report, the main dataset survey. The results of the airflow qualitative assessment are expressed in statistical summaries of the individual features, and enhanced with a sample of the more intriguing observations gleaned from the main dataset time series data. A summary and recommendations conclude the report.

1.1 Army Interest and *WSMR Urban Study* History

Atmospheric urban field measurements are the foundation for extracting repeatable, and thus forecastable, urban atmospheric patterns. These patterns are parameterized into mathematical algorithms, which are then integrated into Army models. The Army models contribute to Army decision aids and become tools for improving military efficiency and effectiveness in the urban environment. (Vaucher et al., 2007)

ARL has been characterizing the airflow and stability patterns around a single building since the first of three field studies was conducted in March 2003. In this *WSMR 2003 Urban Study* (*W03US*) field study, four wind tunnel airflow patterns (Fetch Flow, Velocity Acceleration, Velocity Deficit, and Cavity Flow) were qualitatively verified and the start of a diurnal stability pattern was defined. Two years later, a more detailed study called *WSMR 2005 Urban Study* (*W05US*), qualitatively verified two additional airflow features (Leeside Corner Eddies and Reattachment Zone (RAZ)) and characterized a pattern for the stable conditions around the subject building. (Vaucher et al., 2007)

For additional information on either of these studies refer to Vaucher and Cionco (2004), Vaucher et al. (2006), Vaucher (2006), Vaucher and Cionco (2006), and Vaucher (2007). In section 1.2 in this report, a brief description of the third and latest field study will be given. This later *Study* is the subject of this technical report.

1.2 *WSMR 2007 Urban Study*

W07US was the most ambitious WSMR urban field study of the series. Not only were the various lessons-learned from the previous field studies integrated into the test plan, but the targeted goals for accomplishment were expanded from four to six. These six mission objectives are described in section 1.2.1.

Chronologically, the first significant *W07US* enhancement began with the field study design. Unlike the earlier studies, whose airflow characterization design was based solely on the published Environmental Protection Agency (EPA)/National Oceanic and Atmospheric Administrations (NOAA) wind tunnel results of flow around a single structure of varying proportions (Snyder and Lawson, Jr., 1994), this design utilized both the physical wind tunnel model and computer wind models for placing towers, tripods, and sensors.

Additional *W07US* enhancements included more sensors, improved technology, and a more efficient system for acquiring, processing, and communicating data. The most enriching innovation was the inclusion of the urban disaster response drills, which coincided with the data acquisition. For more details on each of these improvements, see Vaucher et al. (2007).

1.2.1 Mission Objectives

The six *W07US* mission objectives were organized into three general categories: urban characterization research, technological advances, and research applications. The specific objectives were as follows:

Urban Characterization Research:

1. To acquire data for verification of urban micro-meteorology models, such as ARL's diagnostic Three-Dimensional Wind Field (3DWF) model and Los Alamos National Laboratory's (LANL) Quick Urban and Industrial Complex (QUIC) model.
2. To characterize behavior of turbulent airflow around and above a single building.
3. To characterize surface layer stability patterns in an urban environment.

Technological Advances:

4. To design, develop, test, and evaluate an integrated Data Acquisition System (DAS) hardware/software.
5. To evaluate sensor systems for a new mobile, modular, reusable Safari unit design.

Research Applications:

6. To demonstrate disaster response applications for scenarios focused on a single office building.

1.2.2 Test Site Layout and Sensor Selection

The *W07US* test site layout consisted of a subject building with three similar buildings on the north, west, and south sides. To the east was a small, tailored grassy area; a four-row parking lot with a dividing walkway between rows 2 and 3; and a four-lane road. No vehicles were permitted to park in the parking areas during the data acquisition period. Figure 1 displays a plan view of the building domain. This top down view shows the positions for the 12 towers/tripods with respect to the subject and surrounding buildings. Compass north is at the top of the page. The triangles represent the three tower types: 12 m (blue), 10 m (red), and partial 10 m (yellow) towers. The black crosses indicate the 6 m and 2 m tripods. The black dots, surrounding the partial towers on the leeside of the subject building, were fence post positions. Tell-tail flags were attached to each fence post, thus enabling a real time visualization of the circular airflow in that region. The initial location for the aerosol (smoke) release is marked with a cloud-like symbol. The regional prevailing wind was westerly. The local prevailing wind flow went from the southwest to the northeast; thus, the slightly skewed orientation of the major towers.

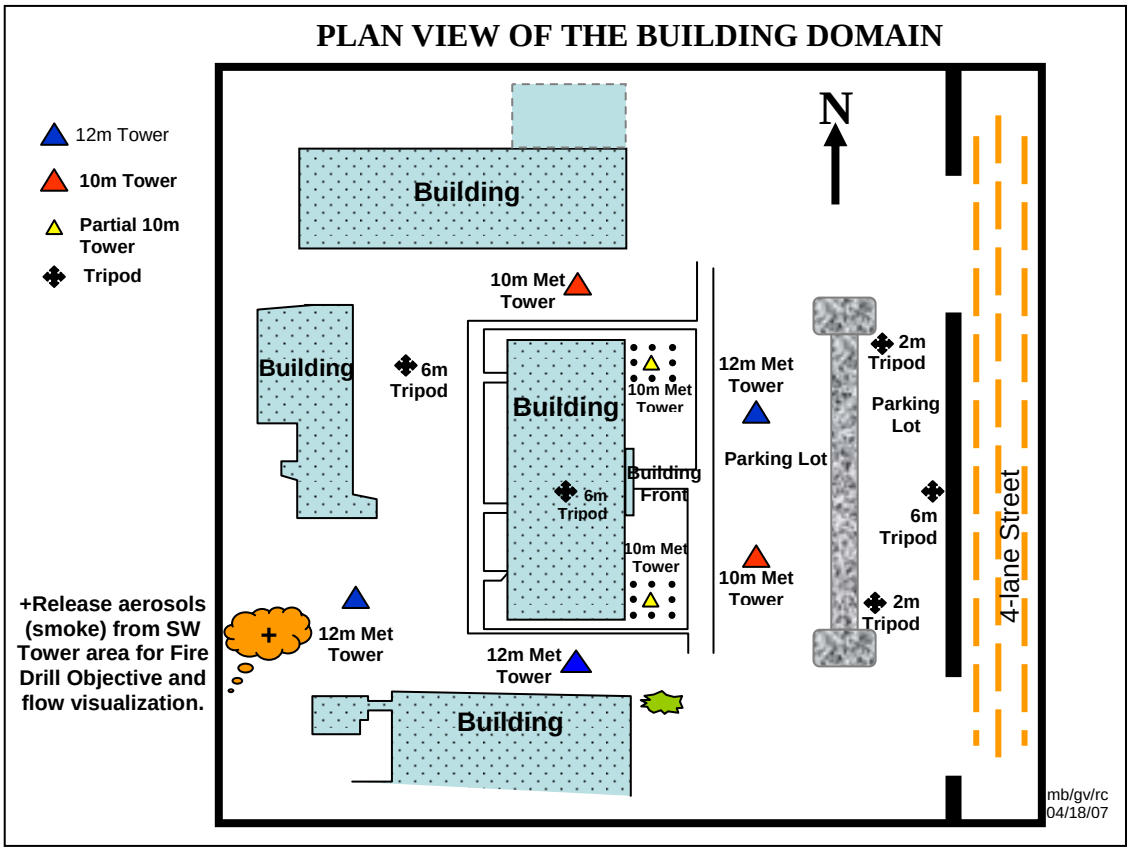

Figure 1. *W07US* test site layout—the black dots surrounding the partial 10 m towers are fence posts with tell-tail flags.

Of the 51 sensors required for this field study, 25 sensors were RM Young Ultrasonic Anemometers (table 1) and 26 were various sensors linked to the Campbell 23X micro-logger (table 2). The Ultrasonic Anemometers or Sonics were selected for their ability to quantify the dynamic characteristics of the urban airflow. These were mounted on the west side of the towers. The Campbell system sensors captured the thermodynamic/stability characterization measurements and were positioned on the east (sunrise side) and south sides of the towers/tripod. The full tower/tripod configuration utilized for both the sonic and Campbell systems is summarized in table 3.

Table 1. *W07US* turbulent airflow measurement information.

Variables	Sensor	Manufacturer	Model
Wind-component vectors, wind speed/wind direction, temperature, speed of sound	Ultrasonic anemometer	RM Young	81000
Wind direction: Located on the northeast and southeast corners of building	Fence post with flag on top		

Table 2. *W07US* mean flow measurements acquired by Campbell CR23X micro-logger systems (Vaucher et al., 2007).

Variable	Sensor	Manufacturer	Model	Units
Pressure	Barometer	Vaisala	PTB-101B	Millibars
Temperature	Thermometer	Campbell	T107	Celsius
Temperature/relative humidity	Thermometer/hygrometer	Vaisala	HMP45AC	Celsius/percent
Wind speed and wind direction	Wind monitor	RM Young	05103	Meter/second, and degrees
Solar radiation	Pyranometer	Kipp/Zonen	CM3	Watts/meter^2
Net solar radiation	Net radiometer	Kipp/Zonen	NR-LITE	Watts/meter^2

Table 3. *W07US* tower configuration.

Tower	Number of Units	Sensors: Sonics (/unit)	System: Campbell (/unit)
12 m tower	3	3 per unit	1 per unit
10 m tower	2	2 per unit	1. North: 1 2. Southeast: 0
Partial tower	2	1. Northeast: 2 2. Southeast: 3	0
6 m tripod	3	1. Roof: 1 2, 3.NWC, RE[a]: 2	1. Roof: 1 2, 3. NWC, RE[a]: 0
2 m tripod	2	1 per unit	0
Totals	12	25 sonic sensors	5 Campbell systems

[a]NWC = northwest canyon; RE = reattachment-east.

Each tower was labeled by the compass position with respect to the subject building. For example, the North tower was north of the subject building. The Southeast tower was southeast of the subject building. Partial towers and tripods were labeled according to the airflow feature being captured and the compass location around the building. For example, the three tripods to the east of the building were called, “Reattachment-North,” “Reattachment-East,” and “Reattachment-South.” For a complete list of the tower/tripod references, see table 4.

Table 4. *W07US* tower/tripod references and sonic heights.

Reference	Tower/Tripod	Sonic Heights
Southwest	12 m tower	2.5, 5, 10 m
South	12 m tower	2.5, 5, 10 m
Northeast	12 m tower	2.5, 5, 10 m
North	10 m tower	2.5, 10 m
Southeast	10 m tower	2.5, 10 m
Roof	6 m tripod	6 m
Reattachment-North	6 m tripod	2.5 m
Reattachment-East	6 m tripod	2.5, 5 m
Reattachment-South	6 m tripod	2.5 m
Leeside Corner Eddy/Vortex-North	10 m partial tower	2.5 east, 2.5 west
Leeside Corner Eddy/Vortex-South	10 m partial tower	2.5 east, 2.5 west, 5 m
Canyon-Northwest	10 m partial tower	2.5, 5 m

1.2.3 ***W07US*** Field Study Design

The *W07US* field study was designed with a four-phase timeline. These phases included the following:

- 2006 July–2007 Mar.: Preparation
- 2007 Feb./Mar.: Pre-*W07US* Calibrations
- 2007 Mar./Apr.: *W07US* Field Portion
- 2007 Apr./May: Post-*W07US* Calibration and *Preliminary Summary* submission

During the Preparation phase, testing was done on the hardware (towers, tripods, etc.), software (DAS, data monitoring, data presentation, etc.), and sensors (tables 1–3). The Pre-*W07US* and Post-*W07US* Calibration phases included side-by-side comparisons of common sensors and running rotations per minute (rpm) and wind direction tests on the wind monitors.

The Field Portion was the actual field study execution. Note: The March data acquisition period was selected for two reasons:

- Southern NM climatology shows the strongest, most consistent winds occur during the March time period. This consistency enabled the field study designers to more accurately forecast tower placement for capturing each airflow feature.
- Solar equinox occurs during March of each year. The equinox's equal heating/cooling cycle within a 24 h period helped to minimize any seasonal bias in the urban stability characterization data.

1.3 *W07US* Reference Material for Additional Information

The *WSMR Urban Study* documentation has been evolving as the original researchers complete their investigations. The current reference materials available to the reader include the following:

1. ARL-TR-4255 (Vol.1): An overview of *W07US* design, preparations, field study execution.
2. ARL-TR-4439 (Vol. DP-1): Data Processing – Pre- and Post- *W07US* sonic calibration.
3. ARL-TR-4441 (Vol. DP-3): Data Processing – airflow qualitative assessment (this report).
4. ARL-TR-4256 (Vol. AS-1): A comparison of stability results from *W03US* and *W05US.*
5. ARL-TR-4452 (Vol. AS-2): Data Processing – stability qualitative assessment, and inter-*Studies* comparison.

2. *W07US* Data Processing

Three of the four *W07US* field study phases involved the acquisition of data. These were Pre-*W07US* Calibration, *W07US* Field Study, and Post-*W07US* Calibration. With 51 sensors acquiring data, the gross data product was about 52 gigabytes (GB) in size (20 GB of calibration data; 32 GB in the main dataset). The data processing effort began at the inception of the field study and continued throughout the field study execution. During the field study, data from each day was logged and evaluated for gross sensor or system failures. Following the data acquisition period, the data processing continued with a more detailed review of the airflow calibration data was undertaken. The results will be published separately in ARL-TR-4439, Volume DP-1 (in publication).

Concurrent with the calibration data analysis, the processing of the large and complex four-dimensional *W07US* main dataset was conducted. The first step in the Post-*W07US* data processing was a survey of the entire main dataset. This survey qualitatively assessed the time-aligned one minute averaged data. The assessment was organized into a series of *W07US* main dataset airflow maps, which served several functions. First, they verified the existence of the original airflow features targeted by the field study design. Second, they summarized each of the airflow pattern's frequency of occurrence for this particular study. And finally, they provided a "quick view" look into the temporal and spatial mapping of each airflow pattern sampled. In short, these qualitative assessment results reduce the large, complicated dataset into a series of manageable *W07US* reference maps, which will be elaborated on in section 3.

Aside: As the astronomer maps space by identifying the various features it contains (galaxies, comets, binary stars, etc.), so have we mapped the *W07US* main dataset with its various features.

3. Main Dataset Qualitative Assessment

The method for mapping the airflow features began by first selecting the specific airflow features expected within the *W07US* main dataset. These features were part of the original *W07US* field study design and consisted of the following:

- Fetch Flow,
- Velocity Acceleration,
- Velocity Deficit,
- Cavity Flows northeast and southeast of the subject building,
- Canyon Flows along the north, south, and west sides of the building,
- Leeside Corner Eddies sampled on the northeast and southeast of the building, and
- RAZ north, east, and south of the subject building.

Step two required well-defined descriptions for each airflow feature. For simplicity, the resources used to identify the airflow features were limited to sonic data. Also, only the most fundamental feature characteristics were translated into airflow pattern identification equations. Table 5 tabulates the resulting resource prerequisites as defined by tower and sonic level(s) references. While this initial investigation considers only the most basic, idealized feature formula, the last three sections to this report suggests alternate variations to future assessments.

Table 5. Fundamental tower/tripod requirements for each airflow feature.

Airflow Feature	Tower/Tripod Used-Number Required Levels	Primary Sensor
Fetch Flow	Southwest-3	Sonics
Velocity Acceleration	Southwest-1, Roof-1	Sonics
Velocity Deficit	Southwest-1, Northeast-1, Southeast-1	Sonics
Cavity Flow	Northeast-3, Southeast-3	Sonics
Canyon Flow	North-2, South-3, Northwest-2	Sonics
Leeside Corner Eddies-Northeast,-Southeast	Northeast-2, Southeast-3	Sonics
RAZ-North, -East, -South	RAZ-North-1, -East-2, -South-1	Sonics

Before utilizing the data resources, the 20 Hz sonic data had to be reduced into 1-min averages. These averages were initially a function of the individual tower and tripod time stamps. However, the inability to accurately inter-compare data across the various towers and tripods quickly prompted the requirement for a standardized, time-aligned, 1-min average to be imposed on all tower and tripod data resources.

A filter to extract only the ideal wind conditions was developed and implemented to simplify future interpretations. This filter capitalized on the field study's test site design, which was based on prevailing winds from the west. In short, the ideal wind direction was defined as 270° (±30°). Where wind speed was a determining factor, the requirement for velocities to be greater than 1 m/s was imposed. This conservative velocity threshold was selected in order to exclude the "calm" atmospheric scenarios of Beaufort Number 0, yet to include conditions where the wind motion would be visible in smoke (Beaufort Number 1) (Wikipedia, 2008a). For flow reversal patterns, the upper level winds followed the westerly requirement and the lower level winds were defined as easterly (90° (±30°)). Variations to this standard are noted in the text, as they apply.

For simplicity, the initial assessment considered each feature independent from neighboring events. Where appropriate, an extended horizontal or vertical airflow pattern was examined for consistencies. In future analyses, the exploration into various possible interactions, dependencies, and correlations between airflow phenomena will be investigated.

In the next seven subsections, each feature is defined, starting with the most critical baseline feature, the Fetch Flow. The order of the subsequent features follows the two general airflow routes built into the *W07US* field study design. Route 1 started with the westerly Fetch Flow, continued eastward accelerating over the building (Velocity Acceleration), then slowed with a Velocity Deficit and Cavity Flow on the leeside of the building (figure 2). The second route began with the westerly Fetch Flow; traveled between/around the subject building (Canyon Flows) and generated Leeside Corner Eddies just after the subject building (figure 3). Finally, after the westerly airflow's interruption by the building, the airflow resumed its westerly path in a RAZ (figure 2). The RAZ can be associated with either route; therefore, this feature will be described last. Figure 4 shows the two routes coincidently.

Note: To help clarify each airflow feature, appendix A presents a cartoon sketch of the seven flow patterns.

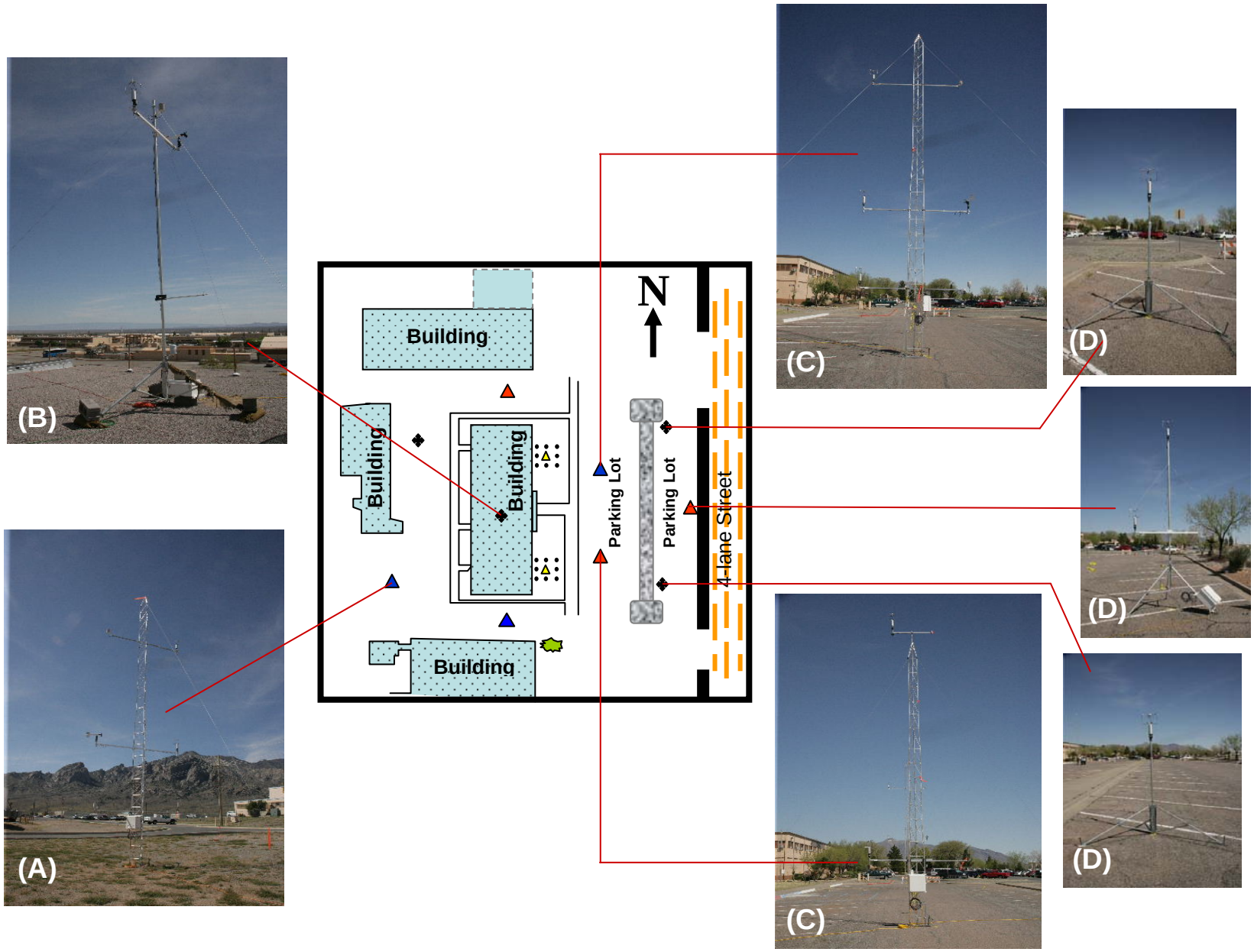

Figure 2. *W07US* flow pattern 1 consists of the Fetch Flow (A) which precedes the building; airflow accelerating over the roof (Velocity Acceleration (B)), then slowing on the building's leeside (Velocity Deficit (C)) and forming a flow reversal (Cavity Flow (C)); and finally, airflow resumes its original character in the RAZ (D).

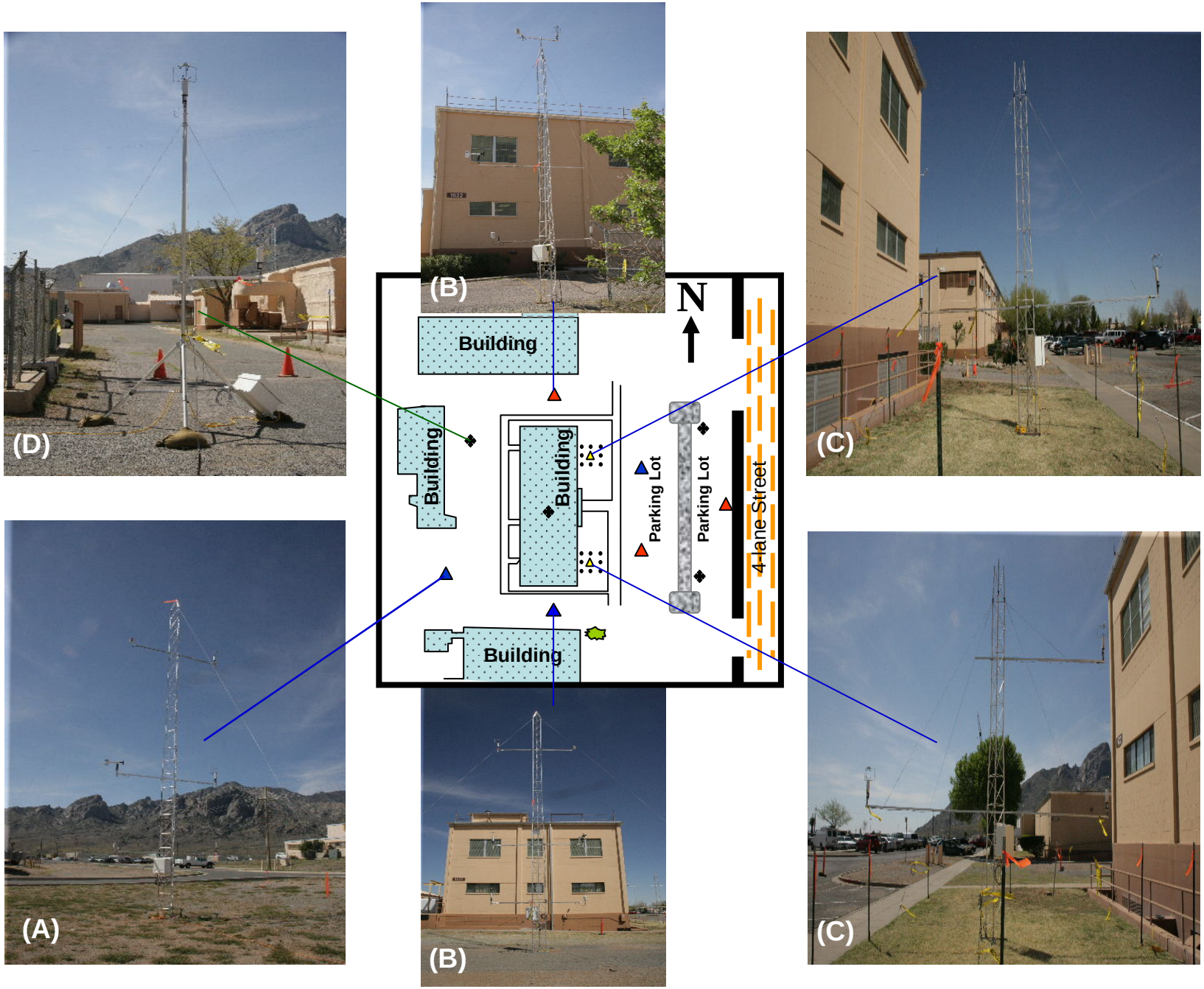

Figure 3. *W07US* flow pattern 2a consists of the Fetch flow (A) preceding the building, the airflow accelerating between buildings (Canyon Flows (B)) and then forming corner eddies/vortices on the building leeside (Leeside Corner Eddies (C)). The *W07US* flow pattern 2b begins with a westerly Fetch Flow then travels along the windward canyon between the buildings (Canyon-West (D)).

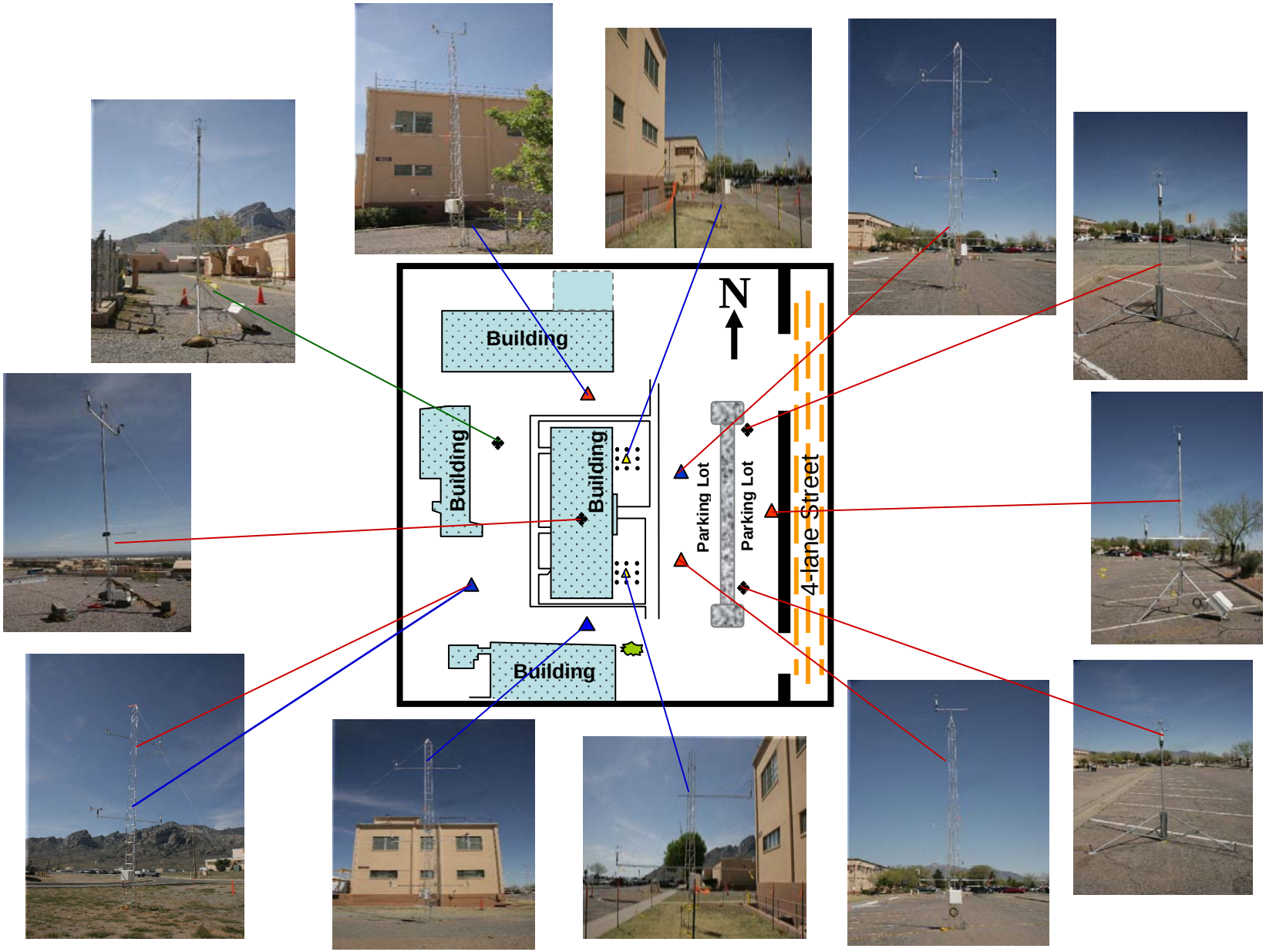

Figure 4. *W07US* field site tower and tripod layout.

3.1 Fetch Flow

The Fetch Flow is the critical cornerstone for the entire single building urban airflow characterization. When the data analysis reaches the point where inter-feature correlations and airflow characterization details are ready for conclusions, nearly all results will have to factor in the character and influence of the pre-building Fetch Flow. Thus, the first feature assessed was the Fetch Flow.

The climatological definition for the ideal Fetch Flow called for westerly winds. Therefore, the *W07US* design placed the Fetch Flow tower aerodynamically upwind of the single subject building on the west side. This original location was based on regional statistics and thus subject to local forcing. The net result was to refine the *W07US* tower position into an open area, west and south of the subject building.

The sonic sensors on the 12 m tall *W07US* Fetch tower were strategically placed at 2.5, 5, and 10 m above ground level (AGL). To ensure an idealized Fetch Flow character, this three-dimensional airflow pattern required all three levels to concurrently be westerly (from 270° ±30°), and greater than 1 m/s. The qualifying 1-min averages were thus identified.

The next question asked was, how long do these westerly inflow conditions need to be sustained for the ideal air mass to cross the entire urban small building complex test site? With a minimum velocity of 1 m/s and considering the maximum distance of this test site, a consecutive 5 min of westerly flow was imposed on the Fetch Flow data. The results showed the average daily occurrences between 10–30 min in length. The maximum occurrence was over 15% of a day in length. (Bustillos, 2008)

3.2 Velocity Acceleration and Deficit as Separate Features

The acceleration of airflow over a flat roofed building followed by a relative velocity drop on the leeside is often correlated into a single event. In this qualitative analysis, the two features were initially examined separately, then together. As an added tool for assessing the nature of the two features, an independent review of the 1-min averaged Fetch Flow feeding these two features was included in the following analysis. Since the Fetch Flow averaging requirements were different, the added tool will be similar but not identical to section 3.1.

3.2.1 Velocity Acceleration

Air flowing over a flat roof with no additional friction-generating obstacles will accelerate (Arya, 2001). The subject building had obstacles on the roof; however, they were not enough to deny the presence of this flow feature. In figure 5, the 1-min averaged data show that Velocity Acceleration (green histogram) was present on all days sampled. The sudden drop in percentage for Julian Date (JD) 81 was due to a power outage on the roof, which ultimately interrupted that day's roof data acquisition.

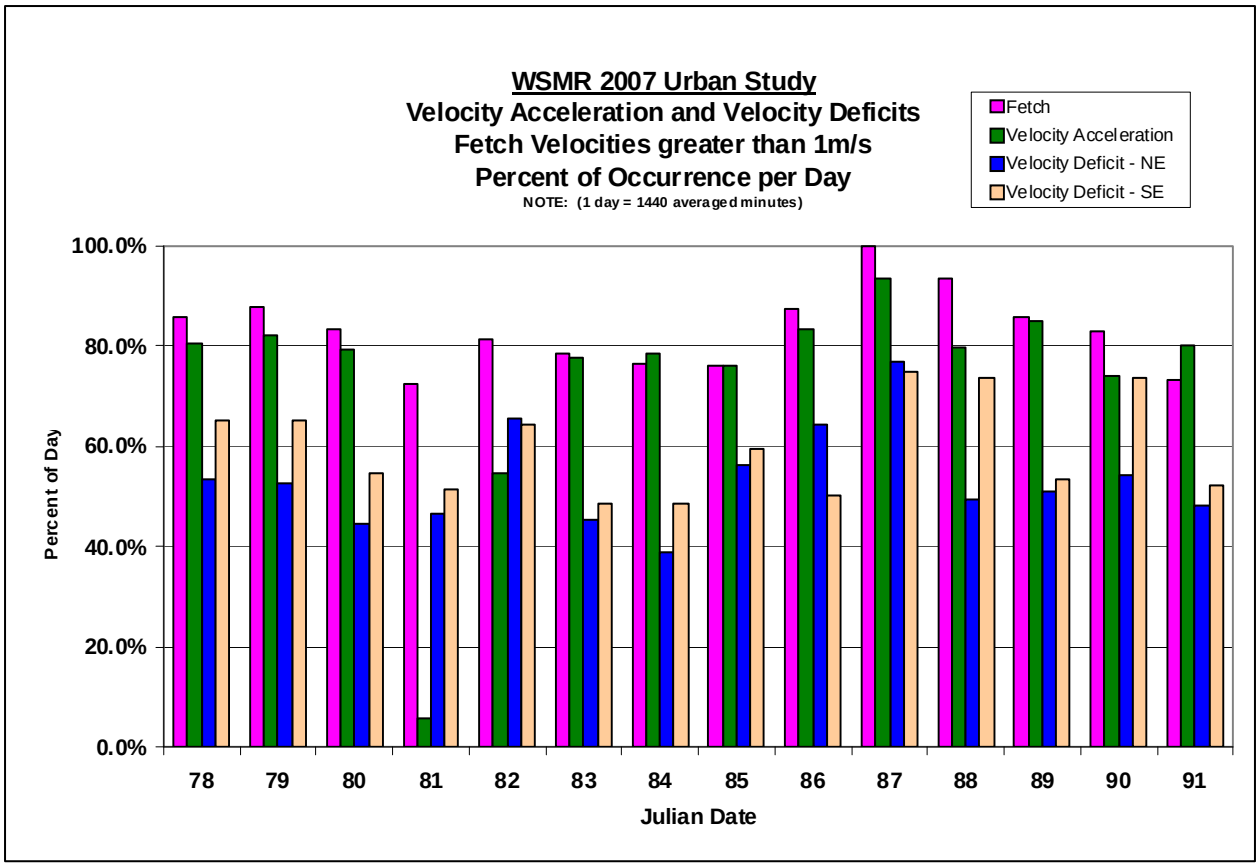

Figure 5. Statistical summary of the individual Fetch Flow, Velocity Acceleration, and Velocity Deficits.

As an interesting contrast, the percentage of minutes for each day in which the reference (Fetch) reported winds greater than 1 m/s is also plotted in figure 5 (pink histogram). (Table 6 summarizes the contrast.) As mentioned above, these values represent those times in which the airflow was greater than "calm" (and is irrespective of the wind direction). While the Fetch velocity and the accelerated roof's flow were not necessarily directly correlated, the Fetch percentage given did provide a qualitative calibrator for the accelerated flows. For all but two days, March 25 and April 1, 2007, the non-calm Fetch showed a greater percentage of time than the Velocity Acceleration. Ignoring a directional dependency, the implication is that when initial winds are greater than calm, this velocity magnitude did not guarantee that there would be acceleration over the roof. In fact, some percentage (usually small) did not generate the feature.

In contrast, consider the two atypical days where the non-calm Fetch reported a lesser percentage than the Velocity Acceleration. The implication is that some "accelerated flow" originated from the calm Southwest tower conditions.

These inconsistent results beg the question of whether the Velocity Acceleration feature has a directional dependency. That is, Velocity Acceleration may still be present, but the airflow source may not be from the west.

Table 6. Percentage of Velocity Acceleration occurrence by day and the percentage of 10 m Fetch wind speeds above 1 m/s per day.

JD	Calendar Date	Velocity Acceleration (Percentage of Day)	10 m AGL Fetch WS > 1m/s (Percentage of Day)
78	Mar. 19	81	86
79	Mar. 20	82	88
80	Mar. 21	79	83
81	Mar. 22	6 (power outage)	72
82	Mar. 23	55	81
83	Mar. 24	78	78
84	Mar. 25	78	76
85	Mar. 26	76	76
86	Mar. 27	83	87
87	Mar. 28	93	100
88	Mar. 29	80	93
89	Mar. 30	85	86
90	Mar. 31	74	83
91	Apr. 1	80	73

Note: WS = wind speed.

On average, the *W07US* daily frequency of occurrence for Velocity Acceleration, as a function of velocity differences only, was 74% (±21%). The maximum occurrence was 93% of a day and the minimum, not counting the day of power outage, was 55% (table 7).

Table 7. Basic statistical results for the Velocity Acceleration and Fetch features during *W07US*.

	Velocity Acceleration (Percentage of Day)	10 m AGL Fetch (Percentage of Day)
Average	74	83
Standard deviation	21	8
Maximum	93	100
Minimum	55 (6 power outage)	72

3.2.2 Velocity Deficit

Airflow on the leeside of a building will slow with respect to the original flow (Fetch) (Arya, 2001). During *W07US*, there were two possible leeside towers from which to evaluate this feature. These were the Northeast and Southeast towers. Both leeside towers were designed with 10 m sonic sensors. To assess this feature, the 10 m Fetch Flow was used as the reference velocity for the wind speed differences. Calculating the differences between the pre- and post-building flows, the Velocity Deficit occurrence was tallied with respect to each sampling day.

Figure 5 shows the results. Each day reported the occurrence of the Velocity Deficit in both the Northeast and Southeast towers. On average, both the Northeast and Southeast towers reported the most fundamental form of the Velocity Deficit feature to occur within 10% of each other (table 8).

Table 8. Basic statistical results for the *W07US* Velocity Deficit-Northeast and -Southeast tower data.

Velocity Deficit	Northeast (Percent of Day)	Southeast (Percent of Day)
Average	53	60
Standard deviation	10	10
Maximum	77	75
Minimum	39	48

Not until the Velocity Acceleration and Deficit (VAD) features are coupled, do these statistics change significantly. This combined pattern will be presented in section 3.3.

3.3 Velocity Acceleration and Deficit as a Continuous Feature

Constructing a continuous pattern to include the VAD features, as well as the requirement that the Fetch exclude "calm" atmospheric conditions, yielded the following three patterns:

- Non-calm Fetch Flow increases velocity over the roof and decreases velocity at the Northeast tower.
- Non-calm Fetch Flow increases velocity over the roof and decreases velocity at the Southeast tower.
- Non-calm Fetch Flow increases velocity over the roof and decreases velocity at both the Northeast and Southeast towers.

Table 9 and figures 5 and 6 present the statistical results for both the individual features and the three continuous over-the-roof flow patterns. On average the occurrence of the first continuous flow ending with the Northeast tower data was about 33% of the day. Pattern 2, ending with the Southeast tower, averaged 38% of the days. The last pattern, involving both leeside data resources averaged 24%.

Table 9. Statistical summary of the VAD.

Aligned		Velocity Acceleration and Deficit [VAD] Dates: 2007 Mar 19-Apr 01						
						VAD(NE)	VAD(SE)	VAD (NE & SE)
		Fetch	Vel Accel	Vel Deficit	Vel Deficit	WS>1m/s, VAD(NE)	WS>1m/s, VAD(SE)	WS>1m/s, VAD (NE and SE)
Julian Date	Date	WS>1m/s % of day	WS Accel Only % of day	NE-Deficit Only % of day	SE-Deficit Only % of day	% of day	% of day	% of day
		SW	*Roof*	*NE*	*SE*	*SW/RR/NE*	*SW/RR/SE*	*SW/RR/NE and SE*
78	070319	85.7%	80.6%	53.4%	64.9%	35.2%	44.9%	28.1%
79	070320	87.7%	82.0%	52.5%	65.1%	37.4%	49.0%	29.5%
80	070321	83.4%	79.1%	44.5%	54.5%	25.3%	34.1%	18.8%
81	070322	72.2%	5.9%	46.6%	51.3%	3.6%	3.5%	2.5%
82	070323	81.3%	54.7%	65.6%	64.3%	36.8%	33.5%	29.8%
83	070324	78.3%	77.5%	45.3%	48.7%	25.6%	26.5%	16.5%
84	070325	76.5%	78.5%	38.8%	48.5%	19.4%	30.0%	14.2%
85	070326	75.9%	76.0%	56.3%	59.3%	33.7%	36.3%	25.4%
86	070327	87.4%	83.1%	64.2%	50.3%	47.8%	35.3%	28.5%
87	070328	100.0%	93.4%	76.7%	74.9%	71.7%	68.5%	48.5%
88	070329	93.3%	79.5%	49.5%	73.5%	34.3%	55.2%	29.9%
89	070330	85.6%	85.0%	51.0%	53.5%	37.0%	39.1%	26.1%
90	070331	82.8%	73.8%	54.1%	73.6%	28.1%	45.2%	23.0%
91	070401	73.1%	80.2%	48.3%	52.1%	27.9%	31.7%	21.9%
	Average:	83.1%	73.5%	53.3%	59.6%	33.1%	38.1%	24.5%
	StdDev	7.7%	21.2%	9.9%	9.7%	15.2%	15.0%	10.3%
	Max:	100.0%	93.4%	76.7%	74.9%	71.7%	68.5%	48.5%
	Min:	72.2%	5.9%	38.8%	48.5%	3.6%	3.5%	2.5%

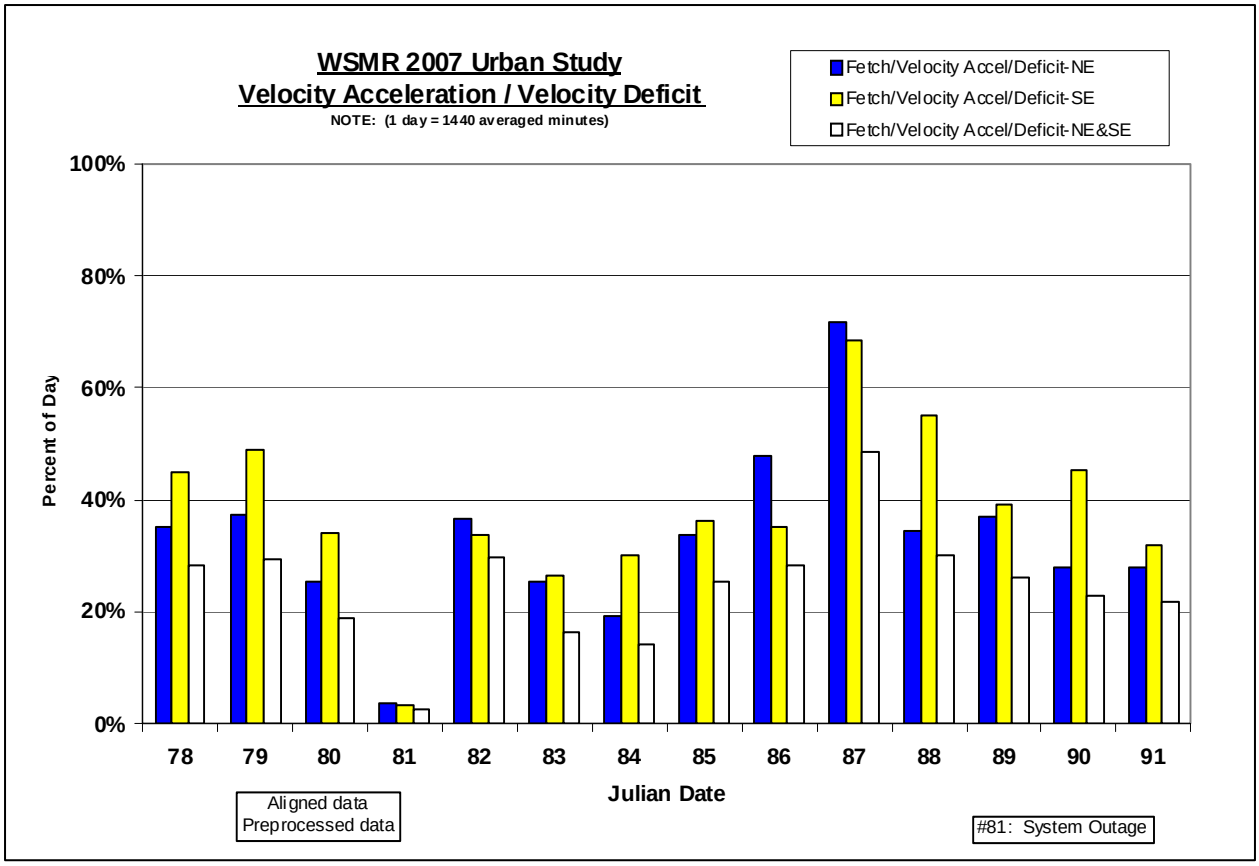

Figure 6. Statistical summary of the three Fetch Flow, Velocity Acceleration, and Velocity Deficit patterns.

Note: JD 81's low percentage was due to a power/system outage.

3.4 Cavity Flow

Cavity Flow, or flow reversal, occurs on the leeside of a building (Arya, 2001). In the *W07US* design, the ideal Cavity Flow pattern was defined as 10 m AGL westerly winds and 2.5 m AGL easterly winds occurring coincidently on the leeside of the subject building. The towers strategically placed to capture this feature included the Northeast and Southeast towers. In the subsequent two subsections, the Cavity Flow attributes of the individual towers will be examined. Expanding these vertical cross-sections horizontally, the final subsection will review the concurrent Northeast and Southeast tower Cavity Flow occurrences.

3.4.1 Northeast Tower Cavity Flow Only

The Northeast tower data reported the upper level westerly flow to occur about four times more frequent (39%) than the easterly lower level flow (10%). The concurrent flow reversal events in the Northeast tower occurred on average about 4% of a *W07US* sampling day. See the blue histogram in figure 7 (also see table 10).

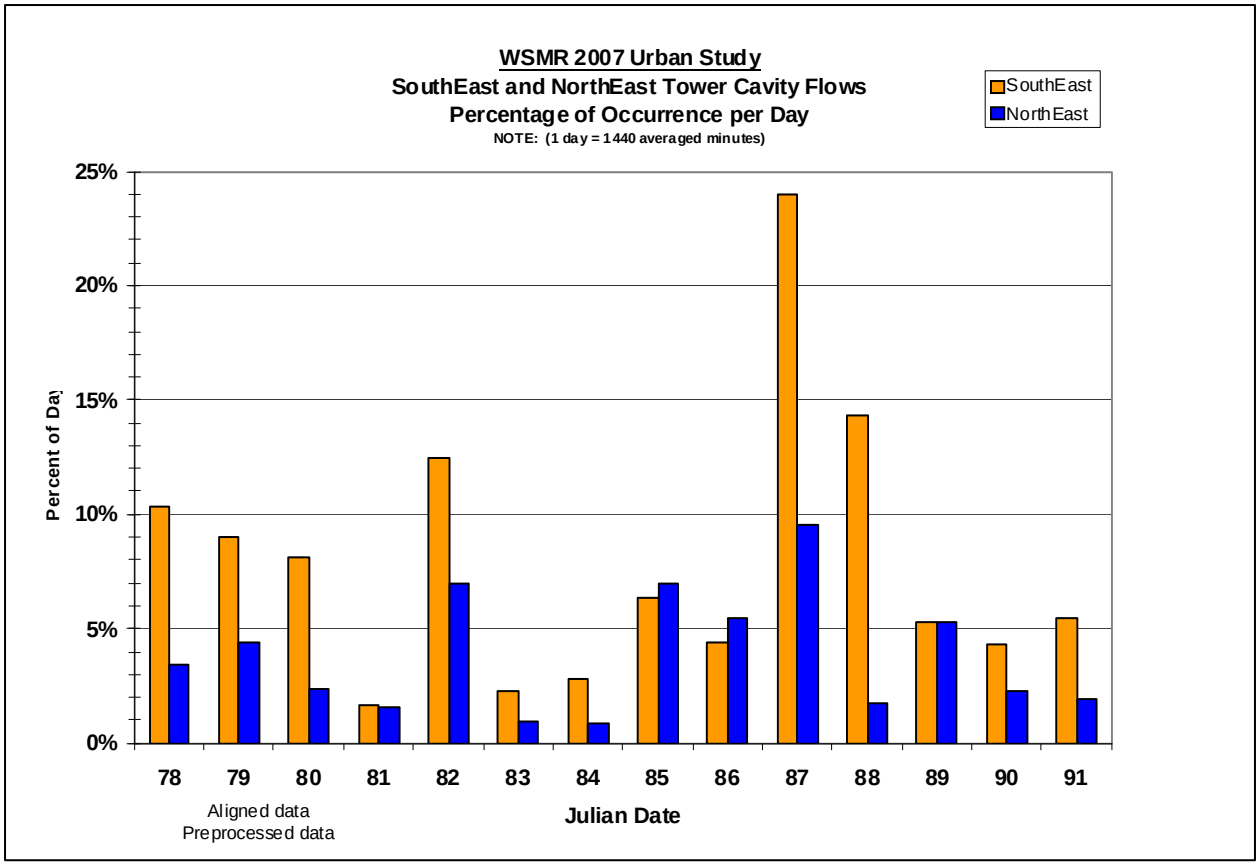

Figure 7. Statistical summary of the individual southeast and northeast Cavity Flows.

Table 10. Statistical summary of the Cavity Flow-Northeast.

Aligned	Tower:	NorthEast		
	Dates:	2007 Mar 19-Apr 01	Westerly	Easterly
	Julian Date	Date	Cavity Flow (% of day)	Upper Level WD (% of day)	Lower Level WD (% of day)
	78	070319	3.4%	46.2%	10.3%
	79	070320	4.4%	38.5%	10.3%
	80	070321	2.4%	29.7%	6.8%
	81	070322	1.5%	17.2%	12.0%
	82	070323	6.9%	44.4%	18.1%
	83	070324	1.0%	21.9%	12.6%
	84	070325	0.8%	20.6%	9.3%
	85	070326	6.9%	39.8%	15.1%
	86	070327	5.5%	43.6%	7.1%
	87	070328	9.5%	86.9%	9.6%
	88	070329	1.7%	56.5%	4.8%
	89	070330	5.3%	35.4%	8.3%
	90	070331	2.3%	34.5%	5.1%
	91	070401	1.9%	29.2%	13.3%
		Average:	3.8%	38.9%	10.2%
		StdDev	2.7%	17.6%	3.8%
		Max:	9.5%	86.9%	18.1%
		Min:	0.8%	17.2%	4.8%

The maximum Cavity Flow-Northeast occurrence coincided with one of *W07US*' most consistently strong windy days, JD 87. Examining the two Cavity Flow contributors individually, the upper level westerly winds showed a maximum occurrence on this same day. The lower level easterly winds, however, reported a slightly less than average percentage. Examining the day on which the lower level easterly flow peaked, JD 82, that same day's upper level westerly flow was only moderately above average for upper level westerly flows. The implied discontinuity of statistics reinforces the need to further explore the local atmospheric dynamics of the individual days before drawing conclusions. In the meantime, statistics showed that all days sampled reported the Cavity Flow feature in the Northeast tower data.

3.4.2 Southeast Tower Cavity Flow Only

The Southeast tower data reported the upper level westerly flow to occur about 2.5 times more frequent than the easterly lower level flow (table 11 and figure 7). When extracting the Cavity Flow pattern from the Southeast tower data, the coincident opposing upper and lower level wind directions averaged about 8% of a sampling day. This is double the frequency of occurrence seen in the Cavity Flow-Northeast statistics.

Table 11. Statistical summary of the Cavity Flow-Southeast.

Aligned	Tower:	SouthEast		
	Dates:	2007 Mar 19-Apr 01	Westerly Upper Level WD (% of day)	Easterly Lower Level WD (% of day)
Julian Date	Date	Cavity Flow (% of day)		
78	070319	10.3%	48.3%	21.4%
79	070320	9.0%	47.2%	19.1%
80	070321	8.1%	32.7%	13.8%
81	070322	1.7%	19.4%	14.6%
82	070323	12.5%	43.1%	26.3%
83	070324	2.3%	23.8%	17.2%
84	070325	2.8%	26.9%	12.1%
85	070326	6.3%	42.6%	13.3%
86	070327	4.4%	32.3%	7.2%
87	070328	24.0%	74.2%	25.3%
88	070329	14.3%	59.9%	19.6%
89	070330	5.3%	35.3%	10.4%
90	070331	4.3%	46.5%	8.8%
91	070401	5.4%	29.2%	20.8%
	Average:	7.9%	40.1%	16.4%
	StdDev	6.0%	14.8%	5.9%
	Max:	24.0%	74.2%	26.3%
	Min:	1.7%	19.4%	7.2%

The maximum daily occurrence of the Cavity Flow-Southeast pattern coincided once again with one of the most consistently strong windy days, JD 87. The upper level westerly winds showed the expected maximum occurrence on this day. The lower level easterly winds reported its second highest occurrence coincidently with the highest easterly flow occurrence (JD 82). As with the Northeast tower data, JD 82's upper level westerly flow was moderately above that level's average for the field study.

3.4.3 Northeast and Southeast Towers Cavity Flows

The final phase of the Cavity Flow assessment was to expand the individual vertical cross-sections into a larger horizontal perspective. To do this, the characteristics of the upper then lower level airflows were explored, after which the coincident Northeast and Southeast tower Cavity Flows were examined.

Horizontally, the upper level westerly flow in the Southeast tower data were present for about the same averaged daily time interval as the Northeast tower upper level westerly winds (40% vs. 39%). The lower level easterly flow in the Northeast lower level showed a slightly lower averaged occurrence than the Southeast tower equivalent.

As explained above, the maximum Cavity Flow occurrence for both Northeast and Southeast towers fell on the same day, JD 87. The upper level westerly winds peaked on this day for both towers. The lower level easterly flow was above average for the Northeast tower and was at the second greatest percentage of occurrences for the Southeast tower. The greatest low level easterly flow occurred on JD 82. The coincident upper level winds from both Northeast and Southeast towers statistically showed a slightly higher than average value for JD 82. Clearly, to understand the dynamics of this feature requires additional information about the local forcing and Fetch Flow attributes.

The coincident Northeast and Southeast tower ideal Cavity Flow statistics were revealing (table 12). On average, less than 1% of a sampling day showed a concurrent flow reversal. Several explanations for this observation will be explored in section 4.

Aligned	Tower: NE & SE Cavity Flows		
	Dates: Mar 19-Apr 01		
	Julian Date	Date	Percent of Day in Joint Cavity Flow
	78	070319	0.8%
	79	070320	0.8%
	80	070321	0.9%
	81	070322	0.1%
	82	070323	0.9%
	83	070324	0.2%
	84	070325	0.3%
	85	070326	0.7%
	86	070327	0.6%
	87	070328	2.4%
	88	070329	0.6%
	89	070330	0.6%
	90	070331	0.6%
	91	070401	0.3%
		Average:	0.7%
		StdDev	0.5%
		Max:	2.4%
		Min:	0.1%

Table 12. Statistical summary of the concurrent Northeast and Southeast tower Cavity Flows.

3.5 Canyon Flow

The most intuitively recognized urban flow feature is the canyon flow between two buildings. The *W07US* design targeted three possible canyon patterns for sampling: a north Canyon Flow, a south Canyon Flow, and a west Canyon Flow. One of the distinguishing features of this flow feature is the vertical stacking of streamlines near or at the midpoint between buildings. For this reason, we chose the assessment requirement that all sampled levels of wind measurements

would be from a single direction parallel to the aligning buildings. In the north and south canyons, this criterion meant that all sampled levels had to show a consistent westerly or easterly orientation. For this assessment, only the westerly orientation was defined as acceptable, since that was the site's prevailing wind direction.

For the North tower, the evaluation involved two levels, and for the South tower there were three levels. The North tower had several manmade and natural obstacles such as a chain-link fence, short bushes, a thin tree, and a couple of utility markers interrupting the airflow. The south canyon had the least amount of local morphological obstacles between the two buildings, namely two staircases (one sub-terrain, one above terrain) and two railings that ran parallel (along wind axis) to each of the channeling buildings.

For the west canyon, this canyon was on the windward side of the subject building and was orthogonal to the prevailing winds of the site. Therefore, the ideal wind flow orientation was either northerly or southerly. Tripod mounted-sonics provided data sampled at two levels (2.5 and 5 m AGL). While the west-canyon tripod was positioned about mid-canyon, southeast of the tripod was a fenced in power pole and utility area which no doubt had an influence on the results.

3.5.1 Canyon Flow-North

To assess the north Canyon Flow pattern, winds from the Fetch, Canyon Flow-North, and RAZ-North areas were considered. Data resources included the Fetch tower (all levels—2.5, 5, and 10 m AGL), the north tower (all levels—2.5 and 10 m AGL), and the RAZ-North tripod (all levels—2.5 m AGL). Time-aligned 1-min averages allowed coincident measurements to be assessed first vertically by the individual sensor-mounting structures, then horizontally, by the three north Canyon Flow pattern structures previously defined.

The vertical assessment yielded the results shown in table 13 and figure 8. Qualifying winds from the Fetch averaged about 28.1% (±15.0%) of the sampled day. The North tower data that fit the criteria averaged 45.5% (±15.3%). The RAZ–North tripod showed an average of 39.4% (±13.6%). Combining the vertical and horizontal westerly winds criteria, these coincident westerly conditions were reported an average of 20.8% (±12.2%) of the sampling day.

Table 13. Statistical summary of the Canyon Flow-North.

Aligned	Towers/Tripod:	Canyon Flow-NORTH
	Date:	2007 Mar 19-Apr 01
	Julian Day:	#78-91
	Avg % of day (all conditions= yes):	20.8%

Julian Date	Date	SW-Fetch Westerly 240<WD<300 All Levels	NN-Canyon Westerly 240<WD<300 All Levels	RN-RAZ Westerly 240<WD<300 All Levels	SW/NN/RN Westerly 240<WD<300
78	070319	31.4%	52.2%	47.0%	21.7%
79	070320	25.3%	47.2%	44.4%	13.5%
80	070321	23.4%	37.2%	33.8%	19.9%
81	070322	12.8%	22.4%	19.6%	8.8%
82	070323	38.9%	48.2%	36.0%	27.4%
83	070324	10.7%	27.1%	23.2%	7.5%
84	070325	10.5%	31.1%	28.9%	7.1%
85	070326	28.6%	49.5%	43.3%	21.5%
86	070327	32.6%	41.0%	28.3%	18.1%
87	070328	69.7%	78.6%	63.5%	53.6%
88	070329	39.0%	68.9%	65.0%	35.4%
89	070330	25.5%	42.6%	36.4%	19.7%
90	070331	23.5%	53.8%	48.5%	18.7%
91	070401	21.7%	36.8%	33.1%	17.6%
	Average:	28.1%	45.5%	39.4%	20.8%
	StdDev:	15.0%	15.3%	13.6%	12.2%
	Max:	69.7%	78.6%	65.0%	53.6%
	Min:	10.5%	22.4%	19.6%	7.1%

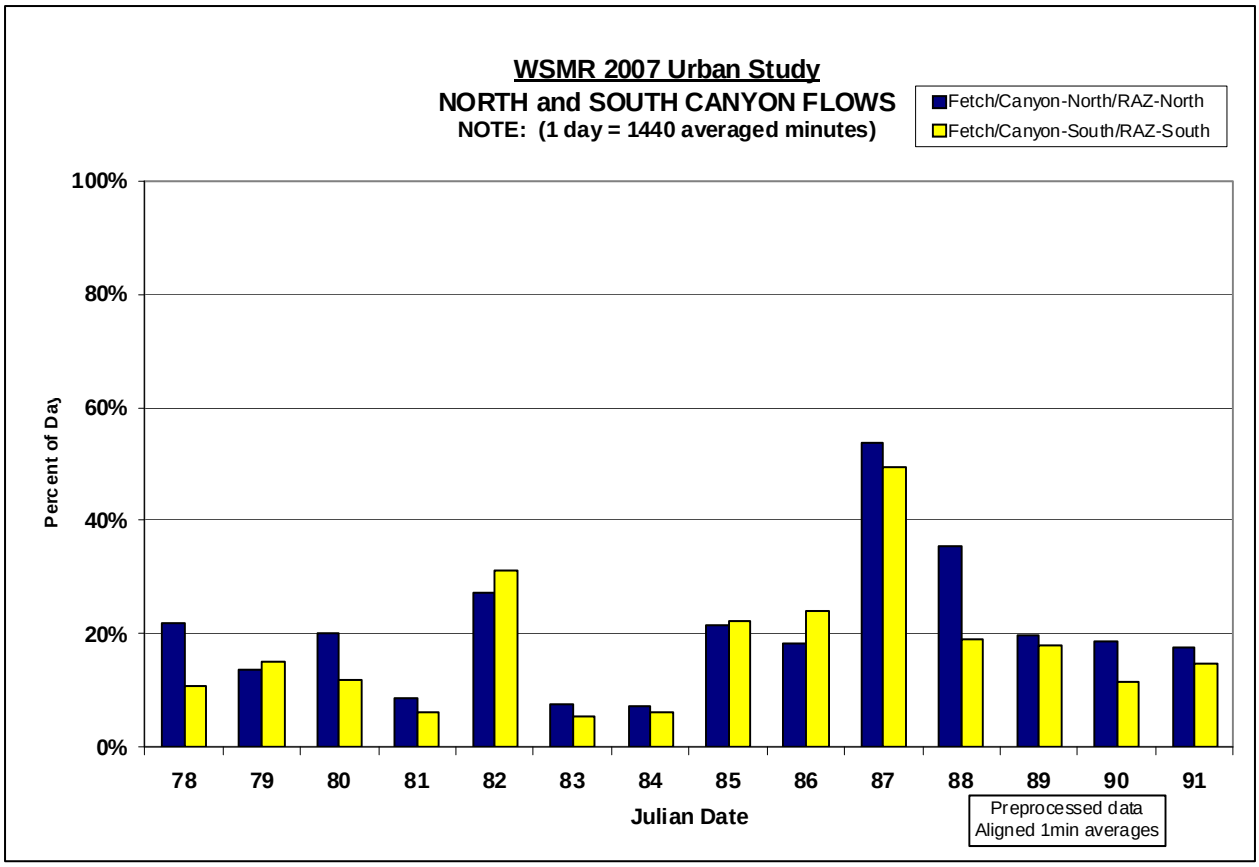

Figure 8. Statistical summary of the Canyon Flow–North and -South patterns.

To better envision the Canyon Flow-North, an educational sample of a data time series used during the above statistical evaluation and the start of the characterization effort has been included in the section 4.

3.5.2 Canyon Flow-South

The south Canyon Flow pattern included winds from the Fetch Flow, Canyon Flow-South, and RAZ-South areas. Data resources included the Fetch tower (all levels—2.5, 5, and 10 m AGL), the South tower (all levels—2.5, 5, and 10 m AGL), and the RAZ-South tripod (all levels—2.5 m AGL). As with the north canyon, the time-aligned 1-min averages allowed coincident measurements to be assessed first vertically by the individual sensor mounting structures, then horizontally, by the three south Canyon Flow-South pattern structures defined above.

The vertical assessment yielded the results shown in table 14 and figure 8. Qualifying winds from the Fetch averaged about 28.1% (±15.0%) of the sampled day. The South tower data that fit the criteria averaged 31.5% (±17.5%), which is 14% less than the north canyon. The RAZ-South tripod showed an average of 26.5% (±11.1%), which is almost 13% lower. Using coincident vertical and horizontal westerly winds as the criteria, an average of 17.6% (±11.8%) of the sampling day was reported. This latter result is approximately 3% less than the Canyon Flow-North.

Table 14. Statistical summary of the Canyon Flow-South.

Aligned	Towers/Tripod:	Canyon Flow - South
	Date:	2007 Mar 19-Apr 01
	Julian Day:	#78-91
	Avg % of day (all conditions= yes):	17.6%

Julian Date	Date	SW-Fetch Westerly 240<WD<300 All Levels	SS-Canyon Westerly 240<WD<300 All Levels	RS-RAZ Westerly 240<WD<300 All Levels	SW/SS/RS Westerly 240<WD<300
78	070319	31.4%	17.8%	30.3%	10.8%
79	070320	25.3%	23.3%	30.1%	15.0%
80	070321	23.4%	26.6%	18.4%	12.0%
81	070322	12.8%	16.6%	12.2%	6.0%
82	070323	38.9%	42.8%	34.1%	31.0%
83	070324	10.7%	17.1%	14.3%	5.4%
84	070325	10.5%	13.3%	14.9%	6.3%
85	070326	28.6%	34.7%	32.0%	22.3%
86	070327	32.6%	44.9%	33.0%	24.2%
87	070328	69.7%	81.1%	54.2%	49.4%
88	070329	39.0%	40.9%	29.5%	19.1%
89	070330	25.5%	30.8%	24.8%	18.0%
90	070331	23.5%	24.6%	16.5%	11.5%
91	070401	21.7%	27.0%	26.7%	14.7%
	Average:	28.1%	31.5%	26.5%	17.6%
	StdDev:	15.0%	17.5%	11.1%	11.8%
	Max:	69.7%	81.1%	54.2%	49.4%
	Min:	10.5%	13.3%	12.2%	5.4%

To better envision the Canyon Flow-South, an educational sample of a data time series used during the above statistical evaluation and the start of the characterization effort has been included in the section 4.

3.5.3 Canyon Flow-West

The west canyon's orthogonal orientation to the prevailing winds required an alternate set of assessment criteria. Namely, ideal air flow could be either northerly or southerly through the canyon. Since the goal of this assessment was to ascertain the frequency of occurrence for this canyon flow type, a decision was made to relax any dependency on the Fetch tower airflow. Therefore, the only criterion for this Canyon Flow-West was that the sampling sensors report a vertically consistent northerly or southerly flow (±30°) from the west canyon tripod sensors (2.5 and 5 m AGL). Any correlation of these results to a Fetch characteristic was left for a follow-on study.

Table 15 and figure 9 show the Canyon Flow-West assessment results. Qualifying southerly flows averaged about 28.0% (±16.4%) of the sampled day. Qualifying northerly flows averaged about half that amount, 14.3% (±7.8%). The cumulative frequency of occurrence for a northerly or southerly canyon flow was therefore, about 42% (±14.8%) (An internal rounding calculation for Mar. 27 is where the tabulated 0.1% difference occurs.)

Table 15. Statistical summary of the Canyon Flow-West.

Aligned	Towers/Tripod:		Canyon Flow-WEST		
	Date:		2007 Mar 19-Apr 01		
	Julian Day:		#78-91		
	Avg % of day:	(Southerly Canyon)	28.0%		
	Avg % of day:	(Northerly Canyon)	14.3%		
	Avg % of day:	Southerly + Northerly	42.3%		
	Julian Date	Date	Southerly Flow 150<WD<210 All Levels	Northerly Flow 330<WD<30 All Levels	ALL Responses All Levels
	78	070319	no NW data	no NW data	no NW data
	79	070320	16.4%	4.2%	20.6%
	80	070321	34.0%	19.5%	53.5%
	81	070322	45.2%	14.7%	59.9%
	82	070323	7.4%	10.9%	18.3%
	83	070324	19.1%	11.7%	30.8%
	84	070325	26.1%	20.6%	46.7%
	85	070326	23.8%	22.4%	46.2%
	86	070327	64.2%	3.8%	67.9%
	87	070328	43.4%	1.3%	44.7%
	88	070329	10.0%	18.5%	28.5%
	89	070330	24.7%	22.9%	47.6%
	90	070331	12.2%	24.1%	36.3%
	91	070401	38.0%	11.8%	49.8%
		Average:	28.0%	14.3%	42.4%
		StdDev	16.4%	7.8%	14.8%
		Max:	64.2%	24.1%	67.9%
		Min:	7.4%	1.3%	18.3%

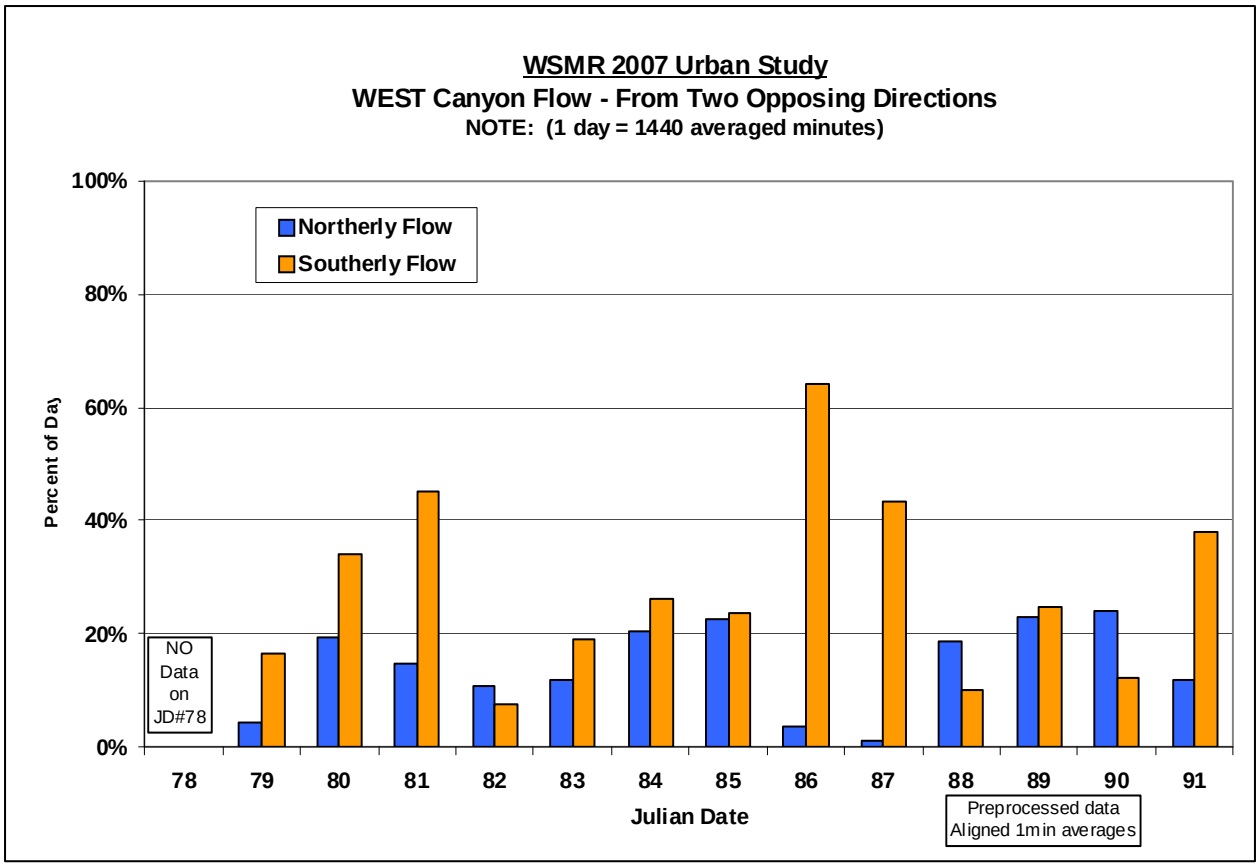

Figure 9. Statistical summary of the northerly and southerly flow directions in the Canyon Flow-West.

3.6 Leeside Corner Eddies or Vortices

Once the canyon airflow has aligned between buildings, the airflow leaving the canyon would subsequently form Leeside Corner Eddies or vortices. The *W07US* design positioned two partial towers to capture the two- and three-dimensional attributes of the Leeside Corner Eddy-Northeast and Leeside Corner Eddy-Southeast, respectively (figure 10). Fence posts with tell-tail flags tied to their tops were planted in a box pattern around the partial towers. The free-floating flags served to visually map the low level (~2 m AGL) air flows.

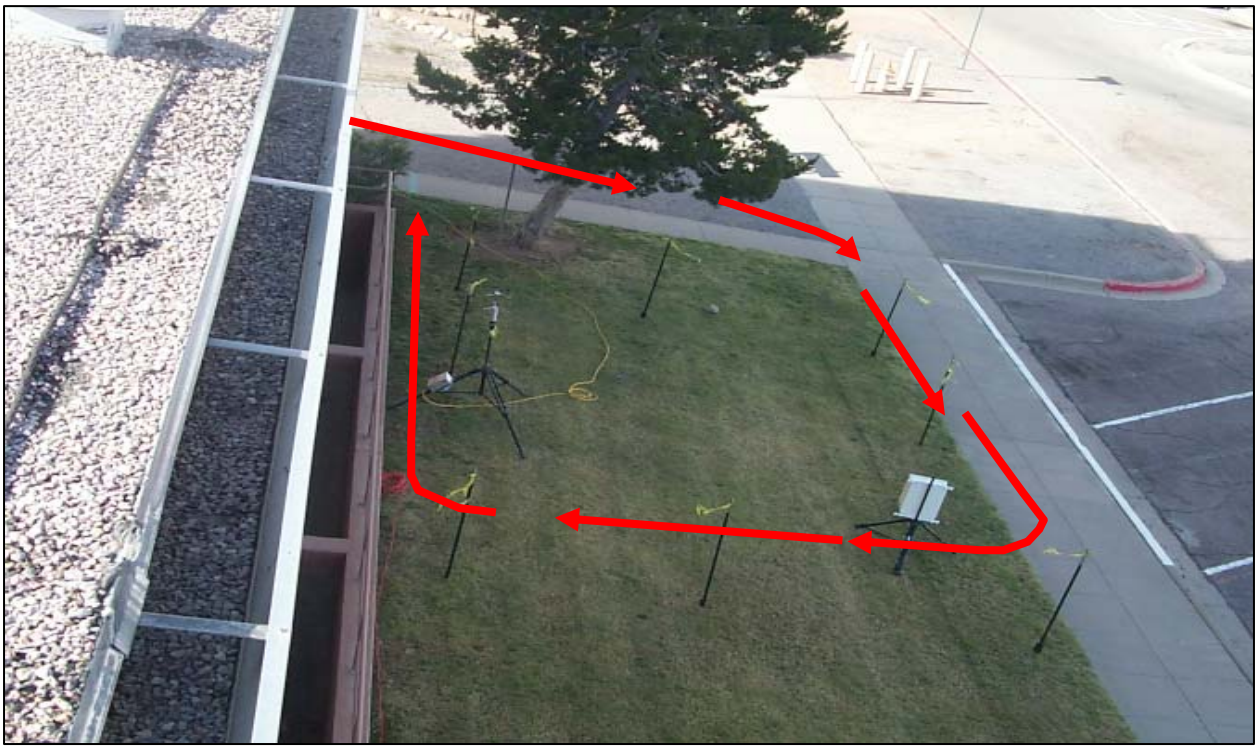

Figure 10. Tell-tail flags on fence posts visually map the Leeside Corner Eddy-Northeast during *W05US*. Notice the proximity of the tree; this tree was removed just prior to *W07US*.

During the field study, smoke was released near the southeast corner and a four-dimensional spiraling pattern emerged. Figure 11 provides a snapshot view of this spiral, giving the participating field scientists additional qualitative experience for mapping the Leeside Corner Eddy patterns.

Figure 11. The *W07US* smoke release maps the Leeside Corner Eddy-Southeast—orange tell-tail flags on fence posts and three mounted sonics also map the Leeside Corner Eddy-Southeast; notice the tree's absence.

In the following qualitative assessments, only the actual vortex pattern itself will be examined. The preceding entrance and subsequent exit air flows were left for a follow-on study. The Leeside Corner Eddy pattern defined as "ideal" starts near the ground and spirals upward.

3.6.1 Leeside Corner Eddy-Northeast

The ideal Leeside Corner Eddy-Northeast starts with a northerly flow at the 2.5 m east side (near the parking lot) position of the vortex. This flow spirals around clockwise, so that equivalent 2.5 m west side (near the building) position reports a southerly flow.

For the *W07US* dataset, the average daily occurrence of a northerly east side sample was 29.8% (±10.3%). The average frequency of occurrence for the return southerly flow was 39.7% (±12.5%). The coincident northerly/southerly flows averaged 2.6% (±1.4%). The results are shown statistically in figure 12. Possible causes for this sharp statistical drop will be addressed in the section 4.

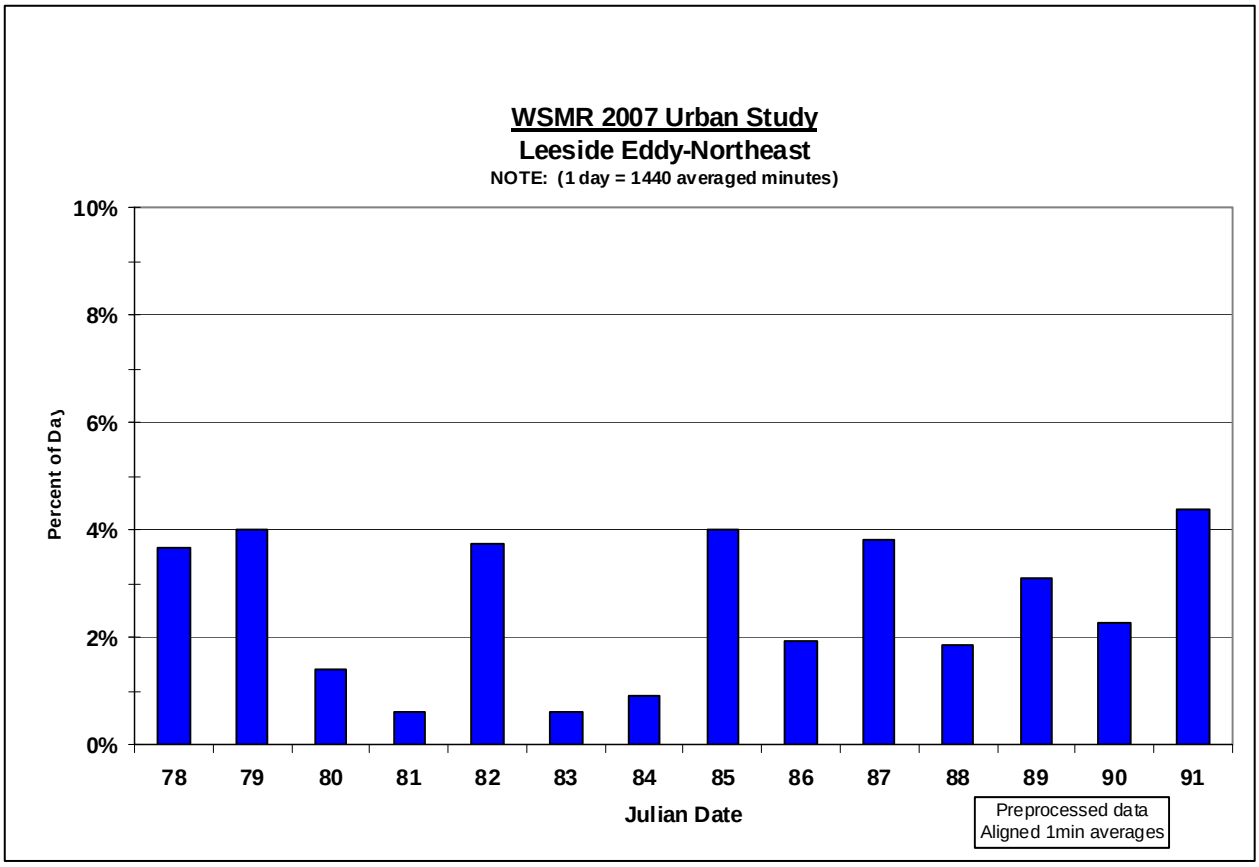

Figure 12. Statistical summary of the coincident northerly (2.5 m-eastside) and southerly (2.5 m-westside) flows around the Leeside Corner Eddy-Northeast.

A standard wind direction tolerance of ±30° was imposed on the assessment. When this tolerance was tightened to ±15°, the northerly and southerly flows both decreased by about 13%. The coincident northerly/southerly flows with this tightened criteria averaged 0.9% (±0.5%).

3.6.2 Leeside Corner Eddy-Southeast

The ideal Leeside Corner Eddy-Southeast starts with a southerly flow at the 2.5 m east side (away from the building) position of the vortex. This flow spirals counterclockwise around a loop, so that the equivalent 2.5 m west side (near the building) position reports a northerly flow. The additional sensor at 5 m on the west side would map a northerly flow, presuming the vertical spiral continues symmetrically (figure A-9).

For the *W07US* dataset, the average daily occurrence of a southerly flow on the east side of the partial tower was 29.3% (±11.0%). The average frequency of occurrence for the lower level return northerly flow was 43.6% (±11.4%). The upper level return northerly flow averaged about 48.1% (±12.5%). The coincident southerly/northerly flows averaged 2.8% (±1.0%). For the daily percentages, see figure 13. Possible causes for the sharp drop in occurrences will be addressed in the section 4.

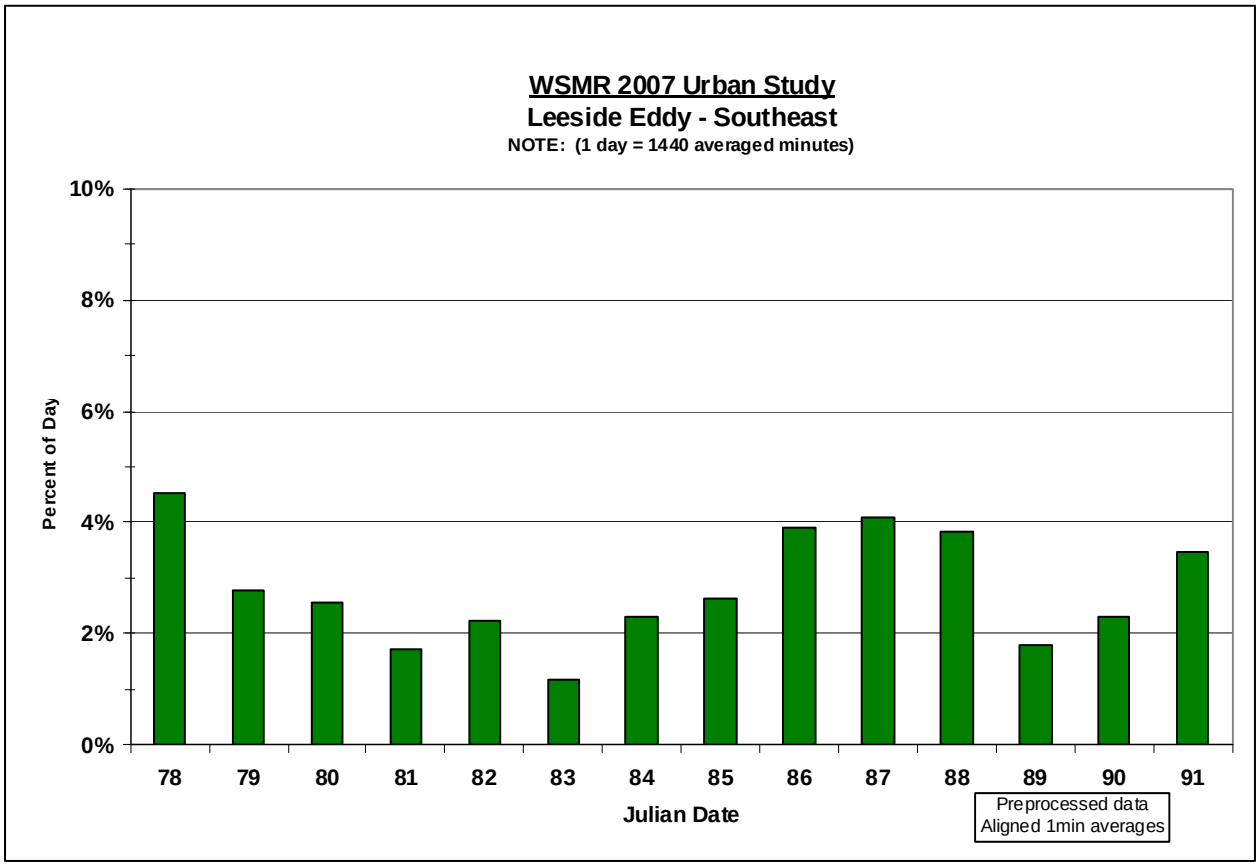

Figure 13. Statistical summary of the coincident southerly (2.5 m-eastside), northerly (2.5 m-westside) and northerly (5 m-eastside) flows around the Leeside Corner Eddy-Southeast.

As with the Leeside Corner Eddy-Northeast, a standard tolerance of ±30° was imposed on the Leeside Corner Eddy-Southeast assessment. When this tolerance was tightened to ±15°, the southerly and northerly flows both dropped about 17%, which is 4% greater than the northeast leeside eddy. The coincident southerly/northerly flows with this tightened criteria averaged 0.6% (±0.4%), which is ~0.3% less than the Leeside Corner Eddy-Northeast.

3.7 Reattachment Zone

Airflow that has gone over or around a subject building will resume its original course in the RAZ. This feature is correlated with the Fetch Flow and is used to represent the start and ending influences of the single building structure on the ambient airflow (figure 14). Since our ideal Fetch Flow was westerly, the ideal RAZ tripod data were required to duplicate this directional flow.

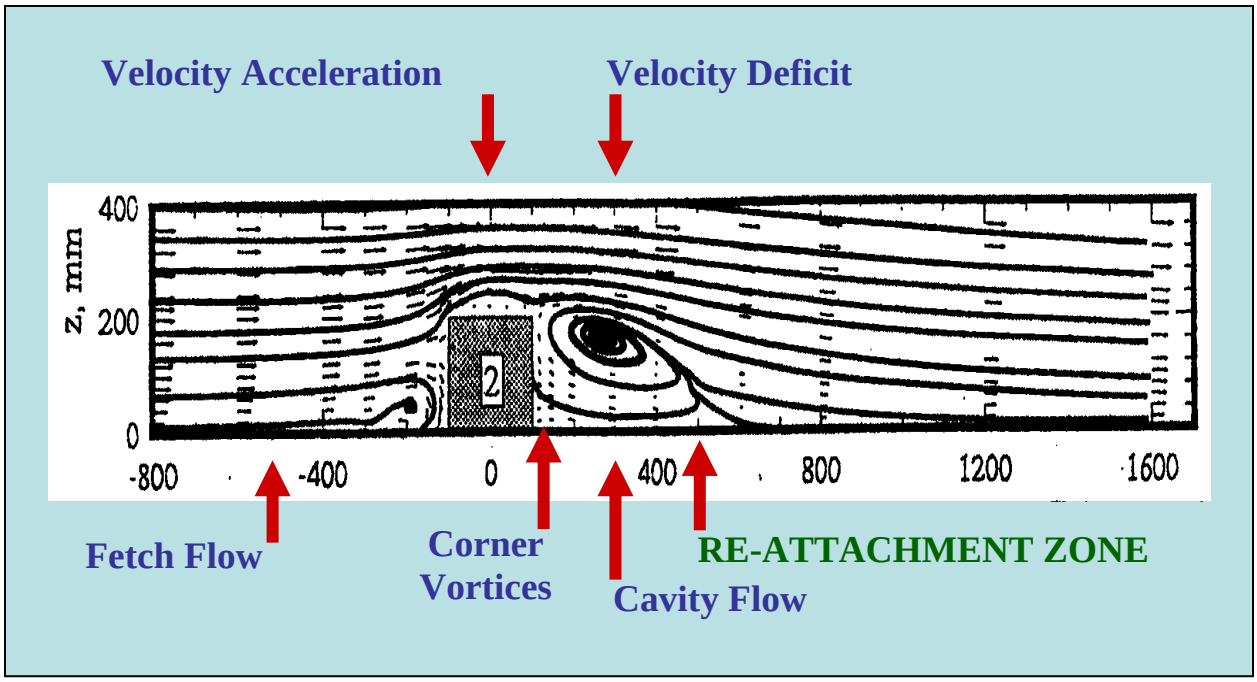

Figure 14. Six flow features observed by the EPA/NOAA wind tunnel (Snyder and Lawson, Jr., 1994); the RAZ feature is labeled in green.

Three independent tripods (north, east, and south) were stationed in positions that represented the leading edge of the RAZ, as defined by the EPA/NOAA wind tunnel studies (Snyder and Lawson, Jr., 1994). The north and south tripods sampled wind data at 2.5 m AGL. The east tripod sampled wind data at 2.5 and 5 m AGL. As with the earlier patterns, this initial assessment began by considering each RAZ resource independent from any other airflow feature. The individual quasi-vertical perspective was then expanded horizontally to include all three positions laterally. The statistical results are summarized in sections 3.7.1–3.7.4, and displayed in table 16.

Table 16. Statistical summary of the RAZ feature.

Aligned							
Reattachment Zone [RAZ]							
Dates: 2007 Mar 19-Apr 01		WD from 240-300 (Deg)	WD from 240-300 (Deg)	WD from 240-300 (Deg)	WD from 240-300 (Deg)	WD from 240-300 (Deg)	WD from 240-300 (Deg)
Julian Date	Date	% of day	% of day	% of day	% of day	% of day	% of day
		All Sonics	RAZ-South	RAZ-East (5&2.5m)	RAZ-East (5m)	RAZ-East (2.5m)	RAZ-North
78	070319	9.0%	30.3%	14.8%	31.0%	17.0%	47.0%
79	070320	10.8%	30.1%	13.5%	25.3%	15.5%	44.4%
80	070321	4.1%	18.4%	7.2%	20.1%	8.2%	33.8%
81	070322	3.8%	12.2%	6.5%	11.5%	7.6%	19.6%
82	070323	3.8%	34.1%	6.2%	22.6%	7.4%	36.0%
83	070324	6.7%	14.3%	10.6%	14.7%	12.4%	23.2%
84	070325	5.7%	14.9%	9.1%	15.2%	11.7%	28.9%
85	070326	9.6%	32.0%	13.0%	22.2%	15.6%	43.3%
86	070327	6.2%	33.0%	9.3%	17.2%	11.3%	28.3%
87	070328	7.8%	54.2%	9.7%	42.5%	10.1%	63.5%
88	070329	11.2%	29.5%	18.1%	39.2%	20.5%	65.0%
89	070330	7.2%	24.8%	11.9%	20.1%	13.8%	36.4%
90	070331	4.8%	16.5%	10.4%	20.6%	13.3%	48.5%
91	070401	8.8%	26.7%	12.7%	21.4%	14.9%	33.1%
	Average:	7.1%	26.5%	10.9%	23.1%	12.8%	39.4%
	StdDev	2.5%	11.1%	3.4%	8.9%	3.8%	13.6%
	Max:	11.2%	54.2%	18.1%	42.5%	20.5%	65.0%
	Min:	3.8%	12.2%	6.2%	11.5%	7.4%	19.6%

3.7.1 Reattachment Zone-North

The RAZ-North consisted of a single sensor which reported westerly flow on average 39.4% (±13.6%) of a sampling day. The maximum occurrence for the westerly flow was 65.0% and occurred on JD 88. The second highest occurrence was on JD 87 at 63.5%. The minimum occurrence was 19.6% and was sampled on JD 81. For the daily RAZ-North statistics, see figure 15.

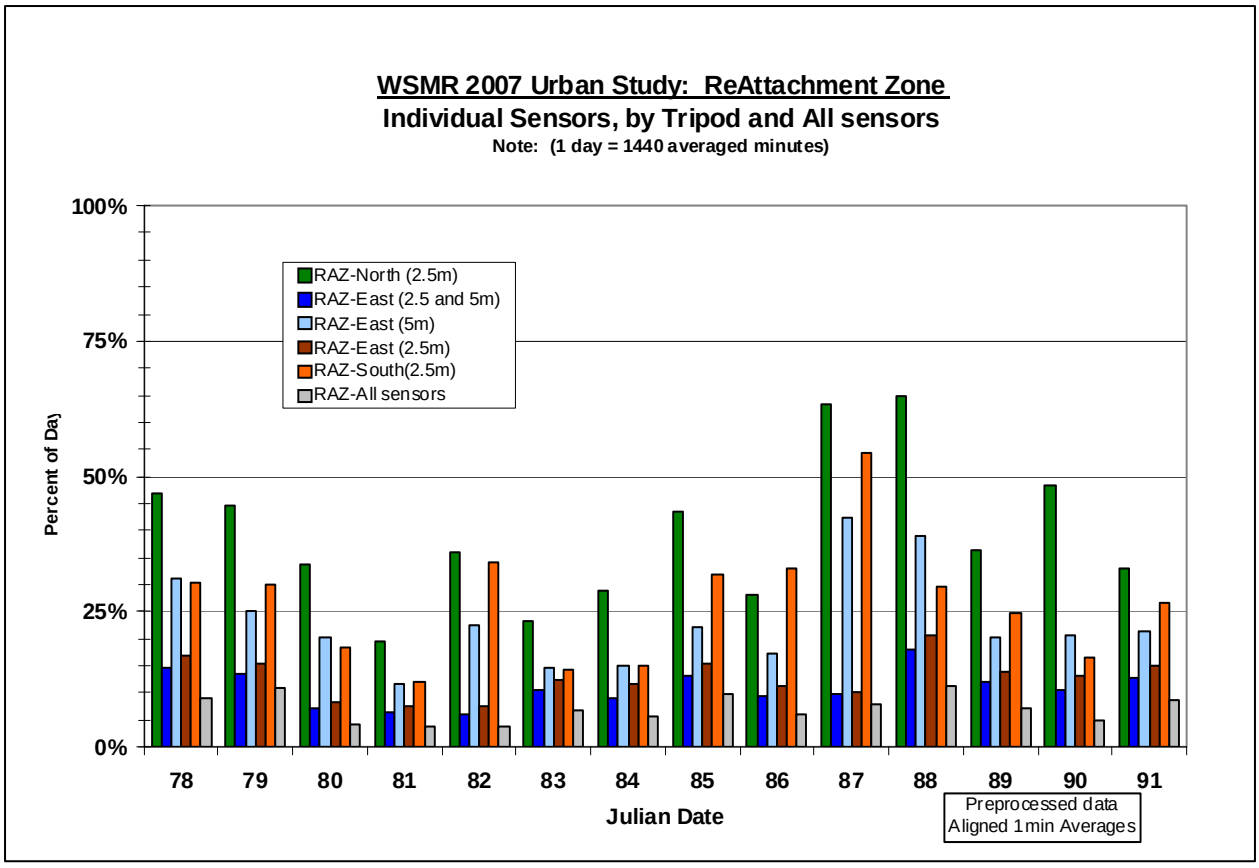

Figure 15. Statistical summary of the RAZ flow by individual sensors, by position (tripod) and, as a horizontally and vertically coincident flow (all sensors).

3.7.2 Reattachment Zone-East

The RAZ-East consisted of a 2.5 and 5 m AGL sensor set, which reported an average occurrence of westerly flow at 12.8% (±3.8%) and 23.1% (±8.9%), respectively. The maximum occurrence at 2.5 m was 20.5% and occurred on JD 88. The maximum occurrence for the 5 m sensor was 42.5% and occurred on JD 87. The 5 m sensor's second greatest occurrence (39.2%) was reported on JD 88.

The minimum occurrence at 2.5 m was 7.4% and occurred on JD 82. The 2.5 m sensor's second least occurrence (7.6%) was reported on JD 81. The minimum occurrence for the 5 m sensor was 11.5% and occurred on JD 81.

The statistics of the coincident 2.5 and 5 m AGL westerly flows showed that the average occurrence was 10.9% (±3.4%). The maximum coincident occurrence was 18.1% on JD 88 and the minimum coincident occurrence was 6.2% on JD 82. JD 81 was the second lowest occurrence. For the daily RAZ-East statistics, see figure 15.

3.7.3 Reattachment Zone-South

The RAZ-South consisted of a single sensor which reported westerly flow on average 26.5% (±11.1%) of a sampling day. The maximum occurrence for the westerly RAZ feature was 54.2% and occurred on JD 87. The minimum occurrence was 12.2% and was sampled on JD 81. For the daily RAZ-South statistics, see figure 15.

3.7.4 Reattachment Zone—A Lateral Perspective

The ideal RAZ feature required all four RAZ sensors to report westerly flow. Statistically, the average occurrence for such conditions was 7.1% (±2.5%) of a sampling day. The maximum occurrence for the horizontally consistent westerly RAZ feature was 11.2% and occurred on JD 88. The minimum occurrence was 3.8% and was sampled on both JD 81 and 82. For the daily coincident RAZ statistics (all sensors), see figure 15.

3.8 Stability

The results of the stability qualitative assessment contained both consistent and inconsistent agreement with the previous two *WSMR Urban Studies*. Elaborating on these results is beyond the design of this technical report; therefore, the stability assessment results are reported in a separate technical report, ARL-TR-4452, Volume AS-2 (Vaucher, 2008).

4. Discussion

The discussion section is intended to highlight key observations and define "next step" suggestions for the ongoing airflow feature analysis and parameterization. In support of the statistical assessment results (section 3), various time series cases were examined. Where these cases reinforce the value in the "next step" recommendations, they are included. These case studies are also good educational materials for instructing the standards and intrigues of urban building air flow patterns.

4.1 Fetch

The most critical feature of the single building urban study is the Fetch. This feature was designed to be a common reference for all other features.

The Fetch assessment began with the ideal atmospheric requirements for a westerly flow ±30°. This criterion was selected based on regional climatological prevailing wind characteristics. Was the wind direction condition appropriate for the *W07US* site during the time of the field study? To answer this question, we peek into a data analysis done concurrently with this assessment whereby the overall Fetch characteristics were examined. While the specific analysis results will be published separately, principle investigator Vaucher statistically confirmed that

the dominant Fetch wind direction during the entire sampling period was westerly (±45°). A very distant second was from the south (±45°), with the north quadrant (±45°) very close behind the second place position. Therefore, the ideal criterion was appropriate for *W07US*.

By design, the initial airflow assessments examined each feature independently. The natural "next step" is to cross-examine the sustained and vertically consistent westerly conditions with each of the other six airflow features. Extending the common Fetch reference concept further, the non-ideal Fetch Flow character (such as a southwesterly flow, southerly flow, etc.) needs to be identified and correlated with each of airflow features examined in section 3. There may be some "downstream" features that suddenly take a dominant presence, once the airflow source is angled from a certain direction. Such results need to be tabulated and if possible, challenged for consistency with equivalent analyses on the earlier *WSMR Urban Studies*.

4.2 Velocity Acceleration and Deficit

The VAD assessment examined these two features (Acceleration and Deficit) independently and as a function of wind speed only. The subsequent evaluation combined the Velocity Acceleration and the Velocity Deficit, but still considered the two Velocity Deficit resources (Northeast and Southeast tower data) separately. A slight increase in the average daily occurrence was observed in the VAD-Southeast pattern, where VAD-Southeast was 38% and VAD–Northeast was 33%. This increase may have been a function of local morphology. The Velocity Acceleration for both the southeast and northeast cases were from the same source and therefore, identical. Thus, the cause for the statistical variations must be with the Velocity Deficit. On the south side of the roof there was a one-story-tall "doghouse" structure. This added obstacle may have created its own mini-VAD environment and subsequently slowed the southeast flow more often than the structurally unobstructed roof preceding the northeast side; thus, creating the statistical results.

When comparing the independent and coincident VAD-Northeast and VAD-Southeast patterns, there was a 10% and greater drop in occurrence for the coincident events. Again, the cause must be with the Velocity Deficit feature, since the acceleration calculations were identical. The unique placement of this same doghouse structure could have created the apparent discontinuity between the leeside Velocity Deficits. That is, with the added height on the south roof, the southeast Velocity Deficit sampler (10 m level) would be more in the shadow of the building rather than in a direct path from the roof flow feature. The unique nature of this southeast micro-environment would function relatively independent from the northeast environment; thus causing a sharp decrease in the coincident VAD statistics.

The "next step" for the VAD analysis is to examine the southeast and northeast VAD patterns independently, but as a function of Fetch wind direction dependencies. Once the dominant characteristics of the two VAD patterns are defined, the current discontinuity between the southeast and northeast Velocity Deficit patterns may be more easily explained.

4.3 Cavity Flows-Northeast and -Southeast

Why was the average coincident Southeast and Northeast tower Cavity Flow pattern less than 1% of a sampled day?

- *Possibility 1—Limited Airflow Resources*: On average the Southeast tower showed a Cavity Flow occurrence of 8% and the Northeast tower showed an average occurrence of 4% (half as frequent). These low percentages were in keeping with the overall low percentages of occurrences reported by all the leeside features observed during the *W07US* data acquisition period. One cause may have stemmed from the atypical seasonal weather conditions that permeated the 14-day data acquisition period. Sustained strong velocities were climatologically forecasted for southern New Mexico in March/April. In the previous two field studies (*W03US* and *W05US*), such weather conditions did prevail. In this *W07US* field study, however, winds were dominated by "light air" (Beaufort Wind Scale) conditions. These systematically slower velocities on the windward side of the building may have been the major cause for the leeside features waning. That is, for lack of airflow resources, the daily frequency occurrences for leeside features were all lower than normal. A natural "next step" then would be to determine if there is a certain wind speed threshold beyond which the leeside features manifest more liberally?

- *Possibility 2—Morphological Influences*: Consistent with the VAD, there was an apparent discontinuity between the southeast and northeast ideal Cavity Flow features. At least two possible causes, both involving morphology are possible: (1) morphology of the roof and (2) a secondary cascaded effect from the re-defined morphology on the building's leeside (removal of two trees).

  Examining the roof morphology, we know that the roof is relatively flat, with the exception of a one-story tall "doghouse" on the south-side. We also observed that the Cavity Flow-Southeast occurred twice as frequently as the Cavity Flow-Northeast. As discussed in the VAD section, perhaps the added building height on the roof's south side formulated a micro-environment. Even with the more frequent slower velocities, the micro-environment may have realigned the roof airflow so as to favor the position of the Southeast tower for the Cavity Flow feature more often than the Northeast tower's location? This south side re-alignment of airflow would then have decoupled the time of feature occurrence and possibly the shape of the Cavity Flow. Thus, the coincident Cavity Flow occurrences would have been statistically reduced.

For the second possible morphological influence on the extremely small coincident cavity flow occurrences, one needs to note the various flow obstacles on the ground level. The original field study design included the effects of two, two-story, mature trees growing on the northeast and southeast leeside corners of the subject building. When these trees were suddenly removed just prior to the field study, the looping signature of the Leeside Corner Eddy changed radically (see section 3.6). Based on improvised flow tracers (white feathers, dust, loose plant brush), the eddy feature became much larger and not entirely symmetric in its looping pattern. Could it be that this eddy's distortion extended into the regions of the Northeast and Southeast towers? If so, this would certainly impact the cavity flow form and frequency. A need to re-examine the interaction of the Leeside Corner Eddy and Cavity Flow is clearly in order.

Finally, the "next step" for the Cavity Flow feature analysis would involve loosening the idealized upper level-westerly/lower level-easterly wind direction criteria. While the "ideal" pattern's frequency of occurrence was substantial, treating each cavity tower resource and each level individually may reveal a "new" leeside Cavity Flow pattern or patterns. In fact, after running various correlations between the upper and lower levels, results may show the flow reversal to be slightly angled, or toppled, in its three-dimensional orientation.

4.4 Canyon Flows-North, -South, and -West

The Canyon Flows were one of the most fascinating features. Statistically, their frequencies of occurrence were not distinctive from the other features. However, when cross-examining these statistics with time series data, some excellent urban airflow tutorial materials were discovered and will be presented later within this subsection. First, we will discuss the along-flow axis canyon features.

The two along-flow canyon features were located to the north and south of the subject building. As explained earlier, a three step horizontal check was defined for the along-flow canyon feature. First, the Fetch needed to be from the west at all levels; second, the Canyon tower data had to be westerly (along-axis); and finally, the RAZ had to show a resumed westerly Fetch pattern. For the statistic assessment, the "ideal" pattern only considered the wind direction as critical. However, when examining the various supportive time series, a second element, namely wind speed, quickly grabs the observant analyst.

Consider JD 87 and the "ideal" north Canyon Flow pattern. In figure 16, the three step ideal north Canyon Flow mapped westerly winds at the Southwest tower (brown), westerly flow at the North tower (green), and a return to the original Fetch Flow's westerly winds by the time the air reached the RAZ-North area (blue). But, this is only part of the story….

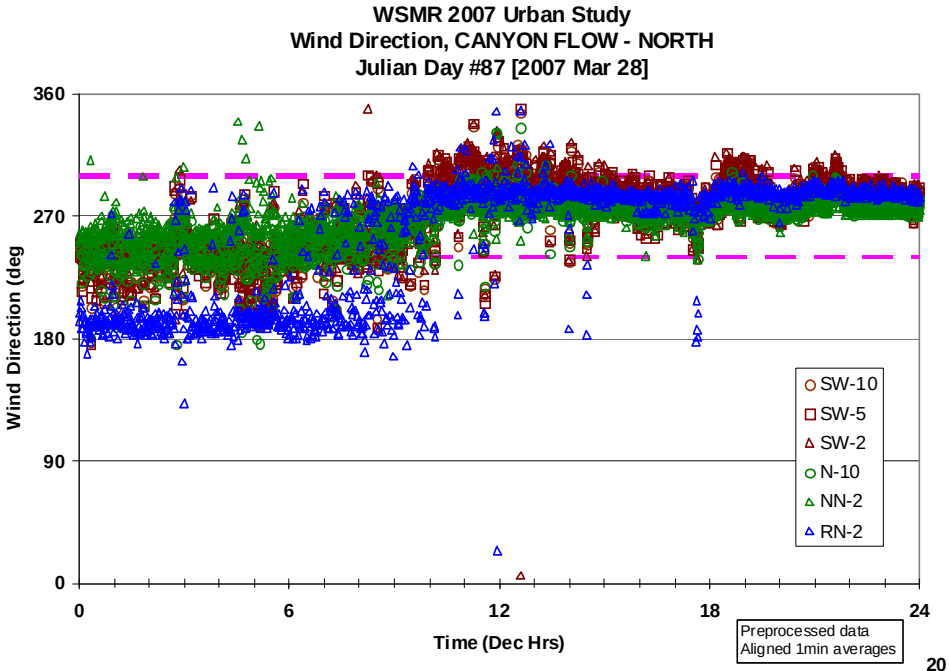

NORTH CANYON FLOW

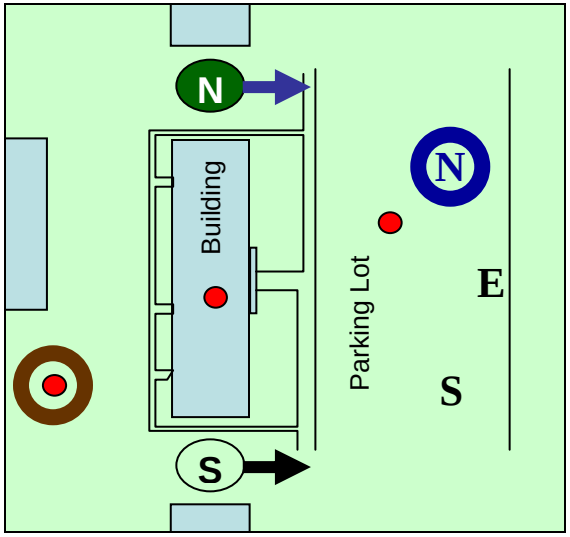

WIND SPEED DURING WESTERLY AIRFLOW IN THE NORTH CANYON

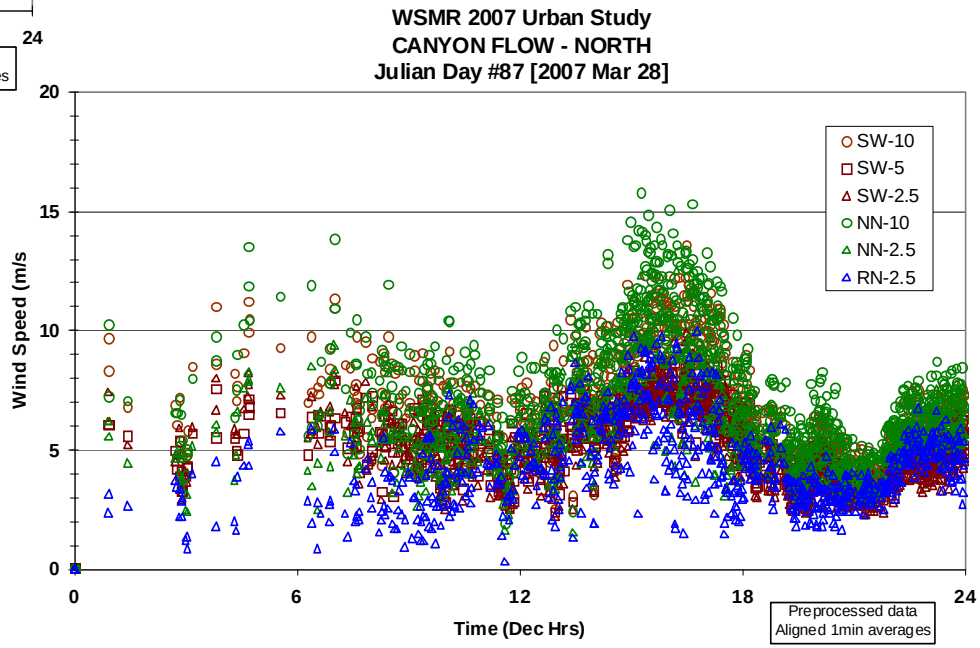

Figure 16. Canyon Flow-North: The ideal Canyon Flow was initially defined as a function of wind direction only. The JD 87 wind speed time series show an acceleration through the North Canyon and a return to original wind speeds at the RAZ-North site.

In figure 16, observe the informative trends in the north canyon wind direction and wind speed time series data from 1200–2400 local time (LT). During this latter half of the day, wind direction (upper left hand graph) is predominantly from the west (ideal). This wind direction will be important when reviewing the south Canyon Flow for the same day. The coincident wind speeds in the lower right-hand graph, show the Fetch tower velocities with brown markers. This Fetch time series is the analysis' reference or, the magnitudes with which we compare the other velocity time series. The north canyon data (green markers) show an accelerated flow with respect to the Fetch velocities. This magnitude increase is in agreement with the Venturi Effect, which explains the accelerated flow through a narrowed path by combining Bernoulli's principle and the equation of continuity (Wikipedia, 2008b). Now observe how the RAZ-North data (blue markers) overlap the fetch velocities. The RAZ was defined as representing the area just outside of the building influence, where the airflow resumes the original, pre-building character. The overlapping Fetch and RAZ wind speed magnitudes between 1200–2400 LT reinforces the basic characteristic of the RAZ beautifully!

Consider JD 87 and the south Canyon Flow pattern (see figure 17). The three step "ideal" south Canyon Flow mapped westerly winds at the Southwest Fetch tower (brown), westerly flow at the South Canyon tower (green), and a return to the original westerly Fetch Flow by the time the air reached the RAZ-South area (blue).

In figure 17, observe the south canyon pattern time series data from 1200–2400 LT on JD 87. The brown Fetch markers show the reference velocities. The green markers for the south canyon data show an accelerated flow with respect to the Fetch velocities. This again agrees with the Venturi effect mentioned previously. The blue markers for the RAZ-South data show a tendency for underestimating the original fetch velocities by about half. Visually inspecting the correlated wind direction, the dominant direction has a northerly component mixed in with the westerly flow. Still working with the wind direction time series data (upper left plot), drop back to the 0000–1000 LT data. Here, a more pure westerly flow seems evident. The coincident wind speed time series shows the RAZ-South velocities to be closer in agreement with the concurrent Fetch time series. This discussion involving the RAZ-South tripod placement and the wind direction will be continued in section 4.6. At this point, however, it is important to note that one of the significant concepts gleaned from the above time series sample is that when one questions whether a wind direction error of 20° is important in an urban environment data set, examples such as in figure 17 show the answer to be a resounding "yes."

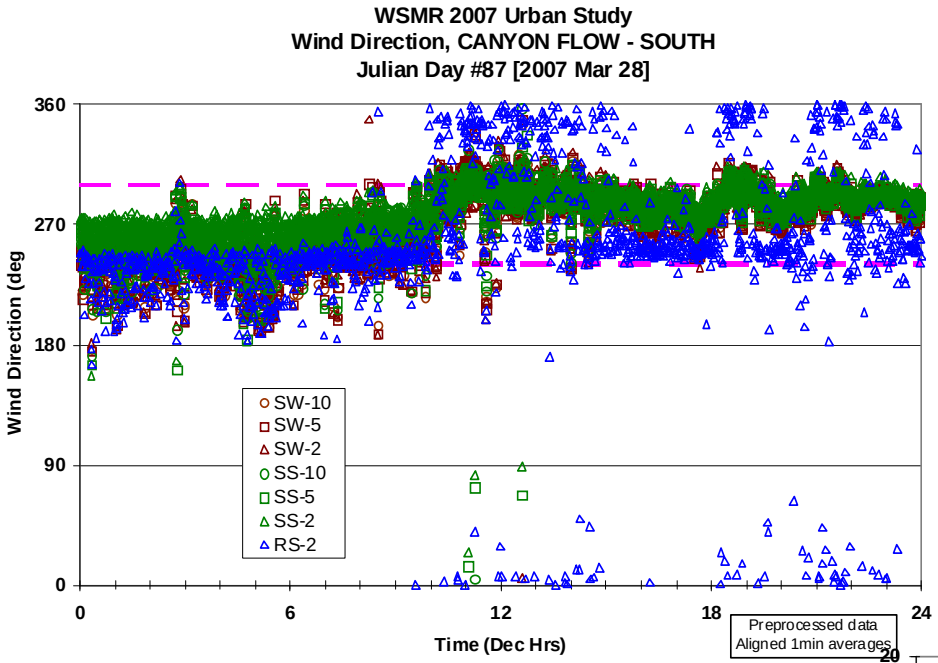

SOUTH CANYON FLOW

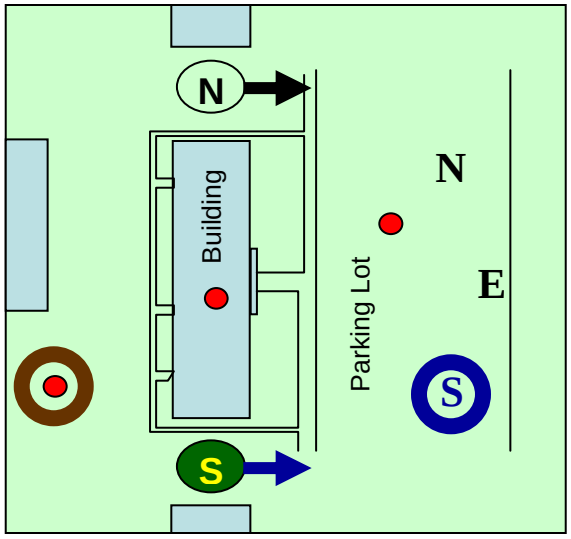

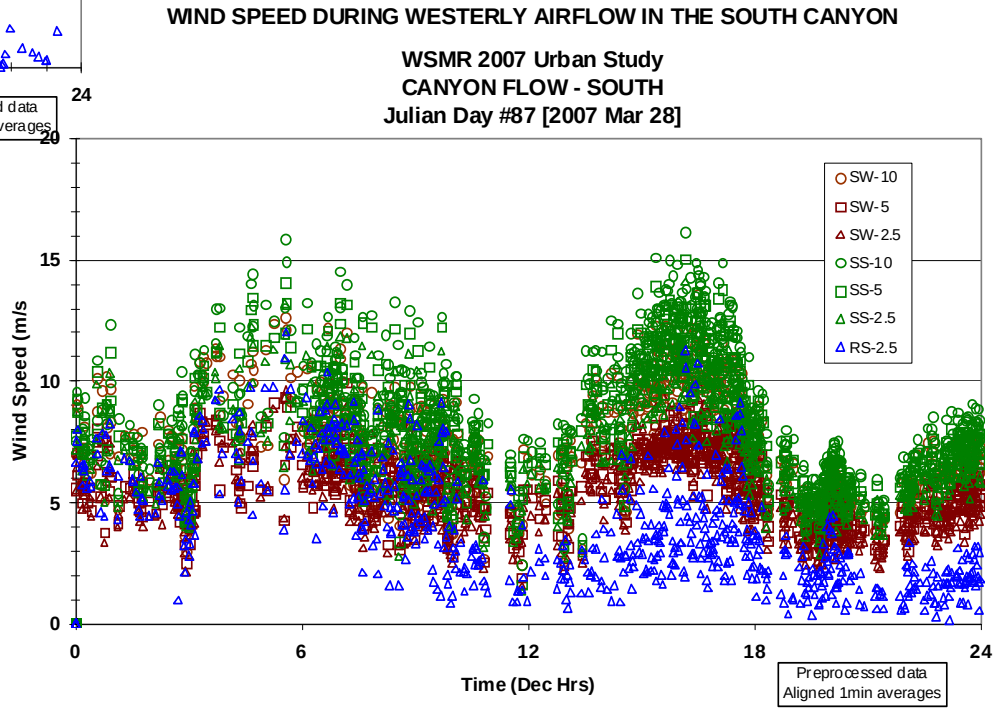

Figure 17. Canyon Flow-South: The ideal Canyon Flow was initially defined as a function of wind direction only. JD 87 wind speed time series show an acceleration through the south canyon and two contrasting RAZ-South characteristics. Prior to 1000 LT, the Fetch and RAZ-South velocities overlap, and after 1200 LT, the RAZ-South underestimates the Fetch implying that the RAZ-South site is still within the influence of the building.

4.5 Leeside Corner Eddies

The Leeside Corner Eddies or vortices are four-dimensional features. Due to sensor resource limitations, the Leeside Eddy on the northeast corner of the building could only be sampled horizontally at 2.5 m AGL. The Leeside Corner Eddy-Southeast had an additional sonic at 5 m AGL, so those data were able to capture a limited view of the vertical, as well as the horizontal structure. The vertical spiral was described in section 3.6 and can be seen in figure 11. Statistically, the frequencies of occurrence for the northeast and southeast Leeside Corner Eddies were fairly similar in magnitudes. The magnitude change of the individual directional flows versus the coincident northerly/southerly flow statistics showed a sharp drop in the concurrent flows. Possible causes for this sharp drop begin with the same cause suggested with the other major leeside feature, the Cavity Flow. That is, the climatological anomaly of having limited strong wind events during the data acquisition period restricted the manifestation of the lesser velocity features such as the corner vortices.

A second possible cause for the sharp drop, and one more directly correlated with the vortex tracking effort, was the sudden, unexpected removal of the two, two-story trees that had been part of the original field design (see section 3.6). Without the trees to filter the flow, the Leeside Corner Eddies seemed to become much larger and were not necessarily concentric. Several qualitative tracking efforts conducted prior to the field study mapped the eddy well into the parking lot area. Though, the qualitative patterns were not consistent, a “best guess” sensor placement had to be implemented within the limited time prior to the data acquisition period. The average daily occurrences of 3% a day does signify that the inner core of the eddy was captured. But, clearly more study needs to be done to better define the arc of each eddy. What can be confidently stated is that the influence of trees next to a building is significant!

4.6 Reattachment Zone-North, -East, and -South

Equally as fascinating as the canyon flow feature was the RAZ. Statistically, the RAZ showed no significant distinction from the other features. However, examining the time series case studies proved very educational.

Returning to JD 87, when the ideal RAZ data were first extracted, the results were those shown in the lower right plot of figure 18. But these ideal westerly conditions really didn’t capture the dynamics of the entire picture. Not until the full time series for JD 87 was examined (upper left plot of figure 18) could one begin to grasp the delicate nature of the RAZ feature. Note in the full wind direction time series, the sudden wind direction shift around 1000 LT. Winds went from a south and southwesterly, to slightly north of westerly. Interpreting this plot, the RAZ-North time series (green) begins southerly from 0000–1000 LT. This might lead one to believe that the south-north aligned subject building was channeling the flow. After the wind shift (1200–2400 LT), the RAZ-North takes a westerly orientation, implying the expected reattachment characteristic.

Examining the concurrent JD 87 RAZ-East, this tripod had two levels, 2.5 (brown) and 5 (blue) m AGL. The 0000–1000 LT shows a vertically consistent southwesterly flow. By afternoon this flow is slightly north of westerly, with the 2.5 m AGL sensor having a slightly more northerly component than its upper sensor counterpart. The interpretation of these two time periods is consistent with the placement of this tripod being slightly further out from the subject building than the neighboring RAZ tripods. The morning data showed the edge of an along-building (channeled) flow, the afternoon data reported the expected RAZ character, with a tendency toward picking up a northerly component presumably from the north Canyon Flow.

Finally, there's the most intriguing JD 87 time series, the RAZ-South data (orange). From 0000–1000 LT, the southwesterly flow is consistent with the RAZ-East data. By the afternoon, the RAZ-South data oscillates continually between northwest and southwest! Interpretation? The atmospheric conditions for that afternoon only were such that the RAZ-South tripod placement must have been within or on the edge of the building's effects, whereas the other two reattachment tripods were placed outside of the building effects in the RAZ. The significance of these JD 87 time series is that the RAZ is not always symmetrical, nor is it stationary.

A study correlating the Fetch conditions with the four-element RAZ data is the natural next step for more accurately capturing the characteristics of the RAZ feature.

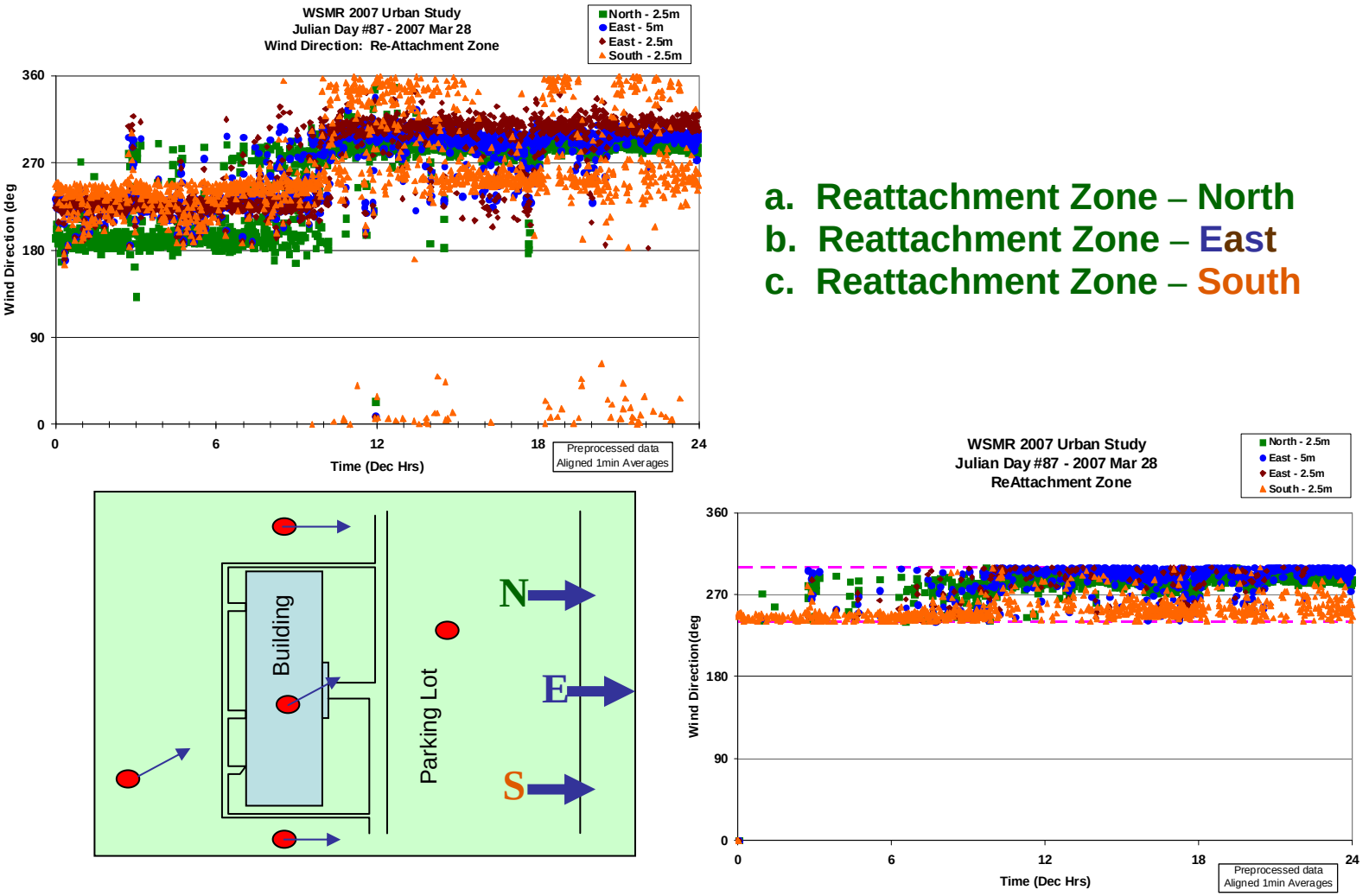

Figure 18. RAZ: The lower right wind direction time series plot shows only the ideal RAZ results for JD 87. The upper left time series shows all JD 87 wind direction data. During the afternoon, the RAZ-North and -East reported expected results. The coincident RAZ-South data showed an oscillating northwesterly-southwesterly pattern, implying that RAZ-South was still within the building's influence during this time period.

5. Conclusion

This first Post-*W07US* main dataset evaluation coincided with the *W07US* calibration data analysis, and has therefore been referred to as a "qualitative assessment." This qualitative assessment reviewed both airflow and stability features targeted by the original field study design. An overview of the stability assessment results was documented in a separate technical report ARL-TR-4452 (Volume AS-2) (Vaucher, 2008).

In this report, the main focus was on seven airflow features in their various locations around and above the single subject building. These features targeted for evaluation by the field study design included: Fetch Flow, Velocity Acceleration, Velocity Deficit, Cavity Flow, Canyon Flow, Leeside Corner Eddies, and RAZ. The approach of identifying features within a massive dataset was explained as being similar to the astronomer's use of stars and star clusters to map the vast heavens. Each airflow feature was defined as a reference point on the multi-dimensional *W07US* main dataset map.

Each feature was initially examined independent of the other features and under the most fundamental ideal conditions. For some features, such as the Cavity Flow and Leeside Corner Eddies, both the vertical and horizontal aspects of the feature were investigated. Other features, such as the VAD and Canyon Flows, required an extended horizontal perspective. All features were statistically tabulated for their frequency of occurrence as scaled by a sampling day. Table 17 summarizes the statistics presented in the previous text.

Table 17. Statistical summary of the *W07US* airflow features.

Airflow Features	Frequency of Occurrence/Day
Velocity Acceleration	NE: 33% SE: 38%
Velocity Deficit	NE: 33% SE: 38%
Cavity Flow-Northeast	NE: 4(±3)%
Cavity Flow-Southeast	SE: 8(±6)%
RAZ-North	N: 39(±14)%
RAZ-East	E: 11(±3)%
RAZ-South	S: 26(±11)%
Canyon Flow-North	N: 21(±12)%
Canyon Flow-South	S: 18(±12)%
Canyon Flow-West	NW: 42(±15)%
Leeside Corner Eddy-Northeast	NE: 3(±-1)%
Leeside Corner Eddy-Southeast	SE: 3(±1)%
	All flow patterns were observed.

Note: E = east, N = north, NE = northeast, NW= northwest, S = south, SE = southeast, and W = west.

All features were verified as present in their ideal form during some portion of each day sampled. Sample cases within the time series data were extracted for further airflow feature verification. While the assessment statistics provided the confidence that each feature was indeed present during each sampling day, the individual time series cases provided a more intimate airflow feature characterization. A sample of the time series cases were presented in this report.

The relatively low frequency of occurrence for the leeside features were explained as a function of atypical climatological wind conditions provided during the data acquisition period, as well as local morphology.

The need to reexamine each feature outside their idealized conditions and to start linking the various features together for their inter-dependencies were suggested as the next steps in the ongoing main dataset analysis. These interdependencies will be a function of meteorological variables such as wind speed, wind direction, and stability, as well as the influence of local morphology. This assessment was just the start of the urban airflow and stability parameterization efforts.

6. Recommendations

Several suggestions were offered throughout the text, especially in the Discussion and Summary sections. Recapping some of these recommendations, the need to re-examine all airflow parameterizations with winds starting above calm levels was suggested. Analyzing each feature under non-ideal westerly fetch conditions was also flagged as a means for bringing "new" airflow feature characteristics to light. Specifically, the need to explore the VAD effects as a function of various wind directions and starting Fetch velocities was given. Regarding the Cavity Flow, the following was suggested: Since the field test design favored local prevailing winds from the southwest, an alternate flow reversal such as southwest-upper and northeast-lower Cavity Flow was flagged for investigation. In contrast, a northwest-upper and southeast-lower Cavity pattern might also be informative. Finally, there were the inter-feature flows, such as the continuous pattern of VAD, Cavity, and RAZ, that were highlighted for future exploration. As pointed out in the Summary, the opportunities for expanding our understanding are just starting.

References

Arya, S. *Intro. to Micrometeorology*, 2nd ed, Intl. Geophysics Series, 79, Academic Press, 2001.

Bustillos, M. Private communication, March 24, 2008.

CNN Web page, *Toxic gas latest insurgent weapon in Iraq*. http://www.cnn.com/2007/WORLD/meast/02/22/iraq.main/index.html (accessed February 22, 2007).

Snyder, W.; Lawson, Jr., R. *Wind-Tunnel Measurements of Flow Fields in the Vicinity of Buildings*, 8th Conference on Applied Air Pollution Meteorology, January 1994.

Vaucher, G.T., White Sands Missile Range Urban Study: *Flow and Stability Around a Single Building, Part 1: Background and Overview*; ARL-TR-3851; U.S. Army Research Laboratory: White Sands Missile Range, NM, July 2006.

Vaucher, G.T. *Urban-Small Building Complex Environment: W07US Stability Analysis and Inter-Study Comparison, Volume AS-2*; ARL-TR-4452; U.S. Army Research Laboratory: White Sands Missile Range, NM, May 2008.

Vaucher, G.T. *Urban-Small Building Complex Environment: Comparing Stable Patterns from Two Similar Urban Field Studies, Volume AS-1*; ARL-TR-4256; U.S. Army Research Laboratory: White Sands Missile Range, NM, September 2007.

Vaucher, G.T.; Brice, R.; D'Arcy, S.; Bustillos, M.; Cionco, R. *White Sands Missile Range 2007 Urban Study: Data Processing - Volume DP-1 (Sonic Calibration)*; ARL-TR-4439; U.S. Army Research Laboratory: White Sands Missile Range, NM, In publication.

Vaucher, G.T.; Bustillos, M.; D'Arcy, S.; Brice, R.; Cionco, R.; Chamberlain, F.; Trammel, J.; Luces, S.; Padilla, R.; Yarbrough, J. *White Sands Missile Range 2007 Urban Study: Flow and Stability Around a Single Building, Volume 1: Field Study Overview*; ARL-TR-4255; U.S. Army Research Laboratory: White Sands Missile Range, NM, September 2007.

Vaucher, G.T.; Cionco, R. *Urban Warfare: Results of a Single building Airflow and Stability Transition Characterization Study*, 72nd MORS Symposium, CA, 2004 June 22-24, 2004.

Vaucher, G.T.; Cionco, R. *Validating a Physical Model with Real Data*, 2006 ITEA Conference, Las Cruces, NM, December 2006.

Vaucher, G.T.; Cionco, R.; Bustillos, M.; D'Arcy, S.; Dumais, B. *Detailing Single Building Stability and Air Flow Patterns (Phase II)*, 6th Symposium on the Urban Environment, AMS, Atlanta, GA, January 29–February 2, 2006.

Wikipedia-the free encyclopedia, *Beauford Wind Scale.* http://en.wikipedia.org/w/index.php?title=Beaufort_scale&printable=yes (accessed January 9, 2008a).

Wikipedia-the free encyclopedia, *Venturi Effect.* http://en.wikipedia.org/wiki/Venturi_effect (accessed March 20, 2008b).

INTENTIONALLY LEFT BLANK.

Appendix A. Airflow Features Schematics

Appendix A shows each airflow feature as a sketched figure. Arrows indicate flow fields, with small consecutive arrows representing quickened motion and larger/longer arrows indicating slower motion. Site layouts are not drawn to scale.

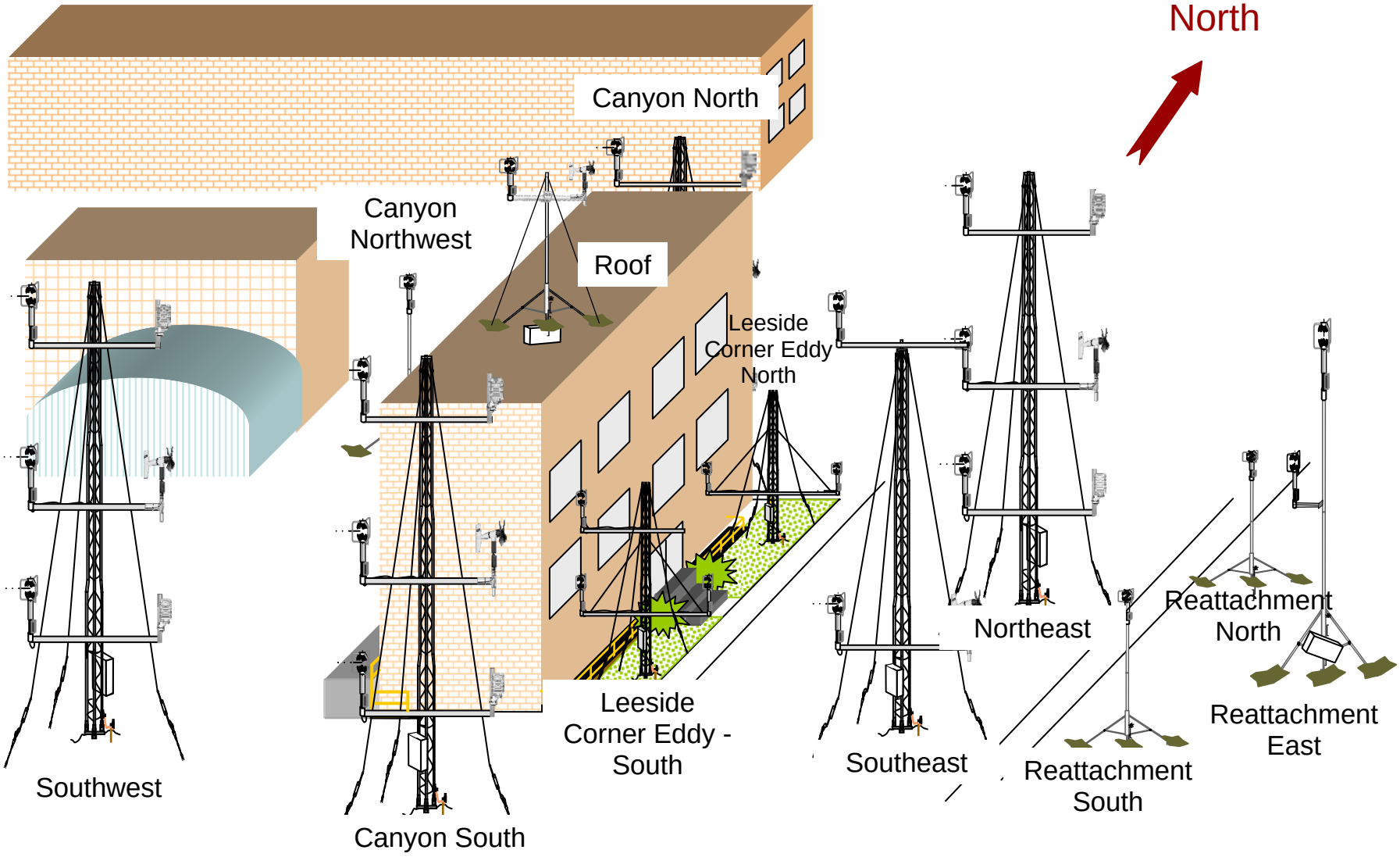

Figure A-1. *W07US* field study site schematic, including the 12 towers and tripods site names.

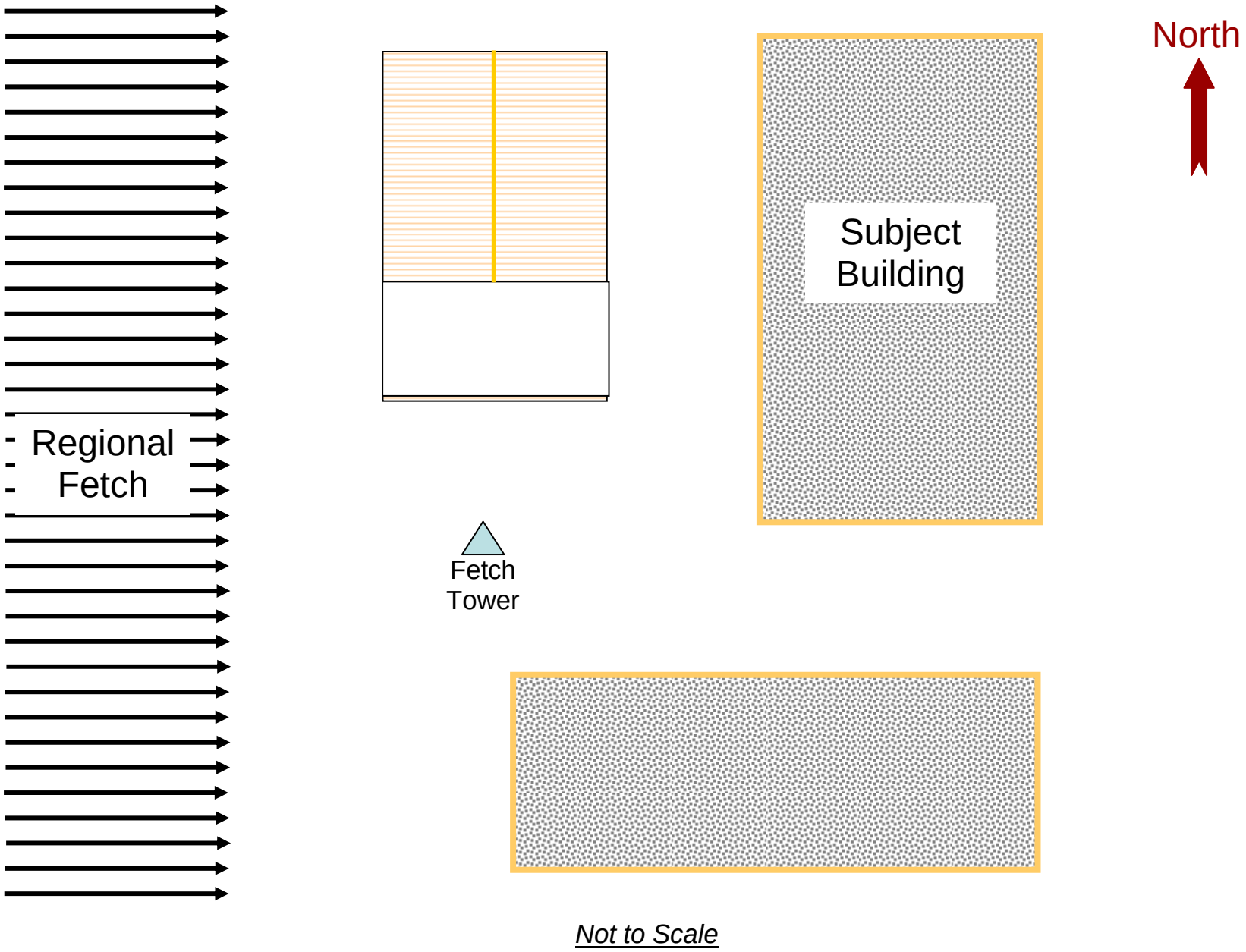

Figure A-2. *W07US* field study site schematic; the westerly regional Fetch Flow is indicated by the multiple long black arrows.

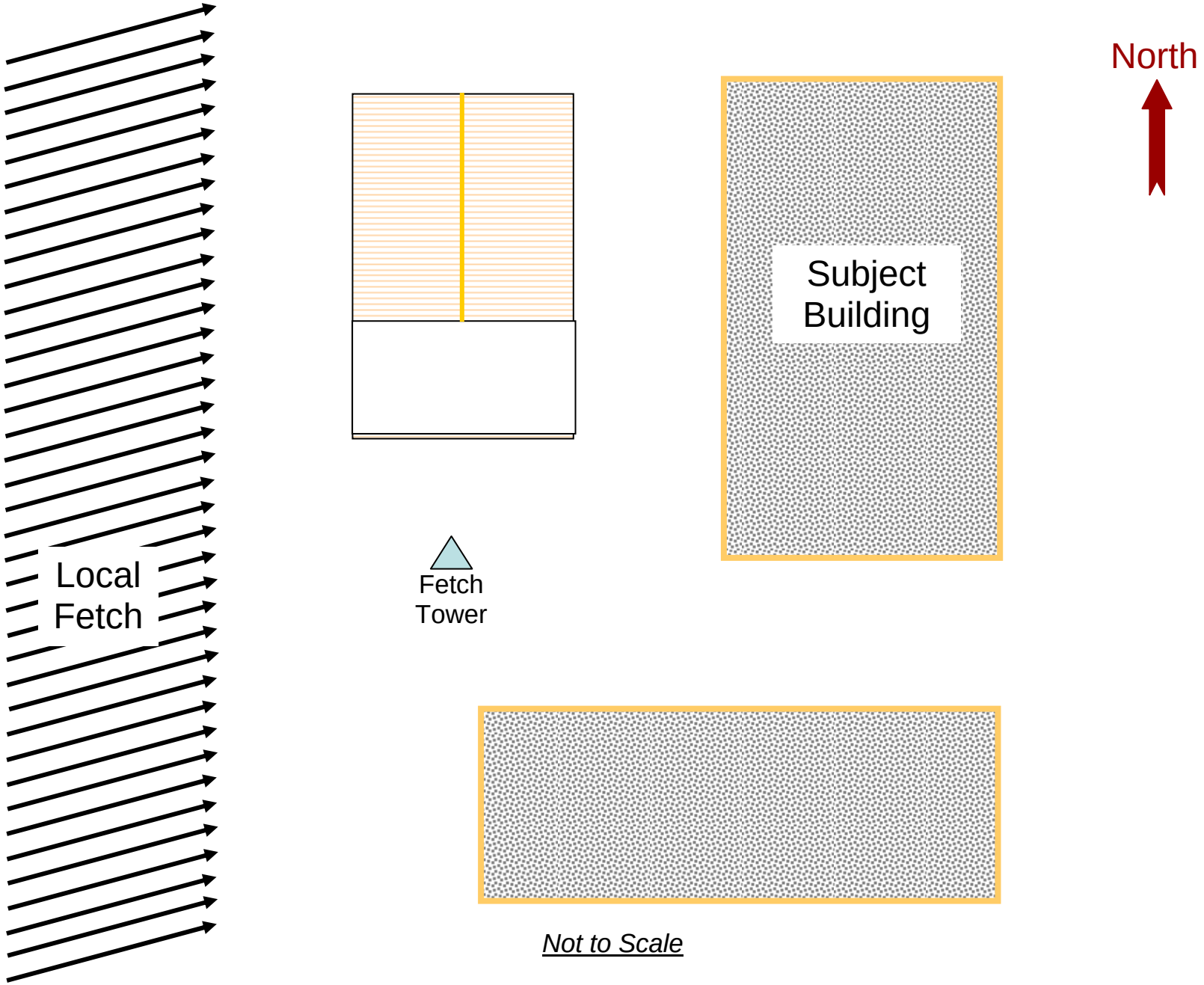

Figure A-3. *W07US* field study site schematic; the southwesterly local Fetch Flow is indicated by the multiple long black arrows.

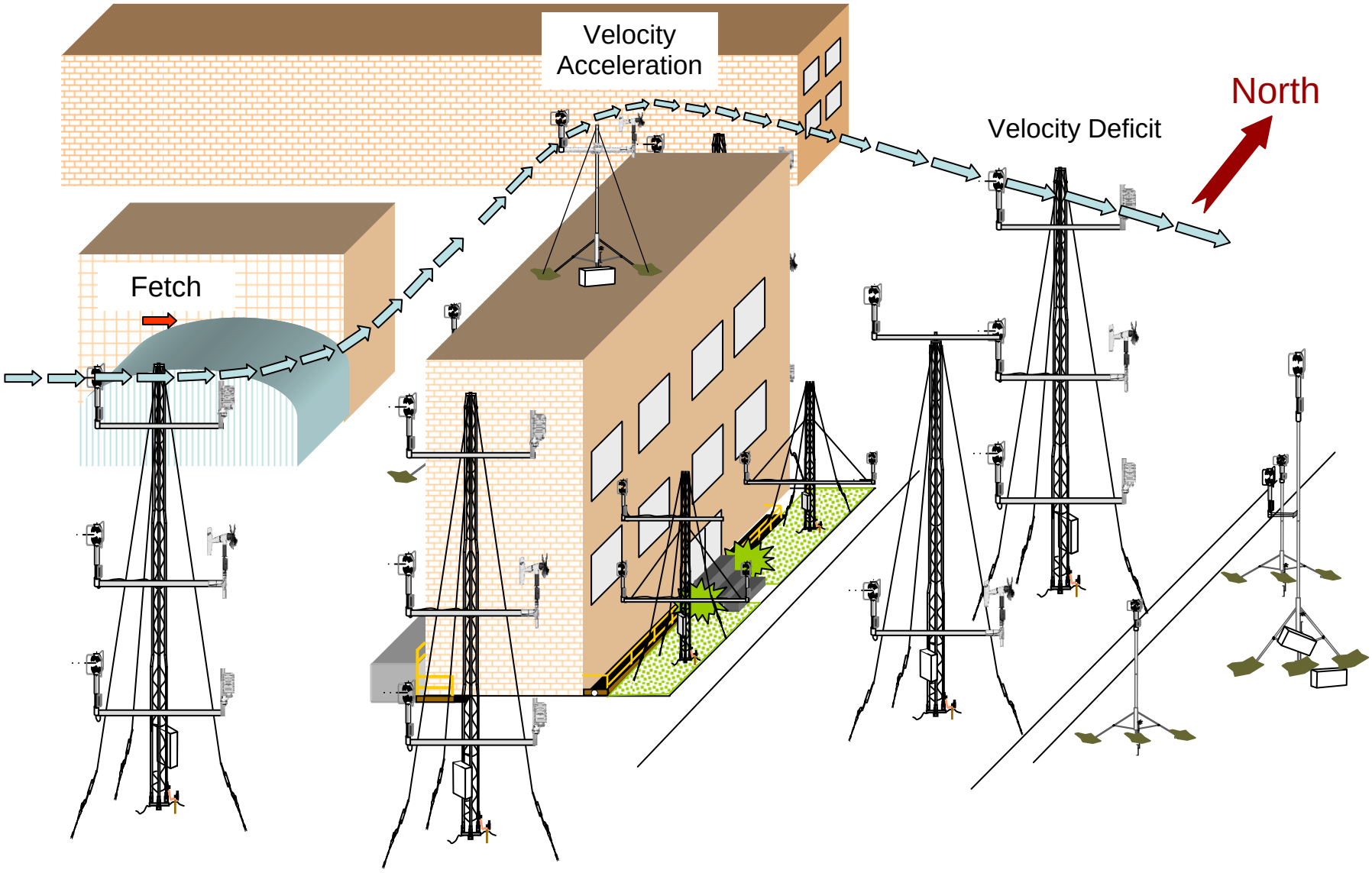

Figure A-4. Schematic of the *W07US* Fetch, Velocity Acceleration, and Velocity Deficit airflow features.

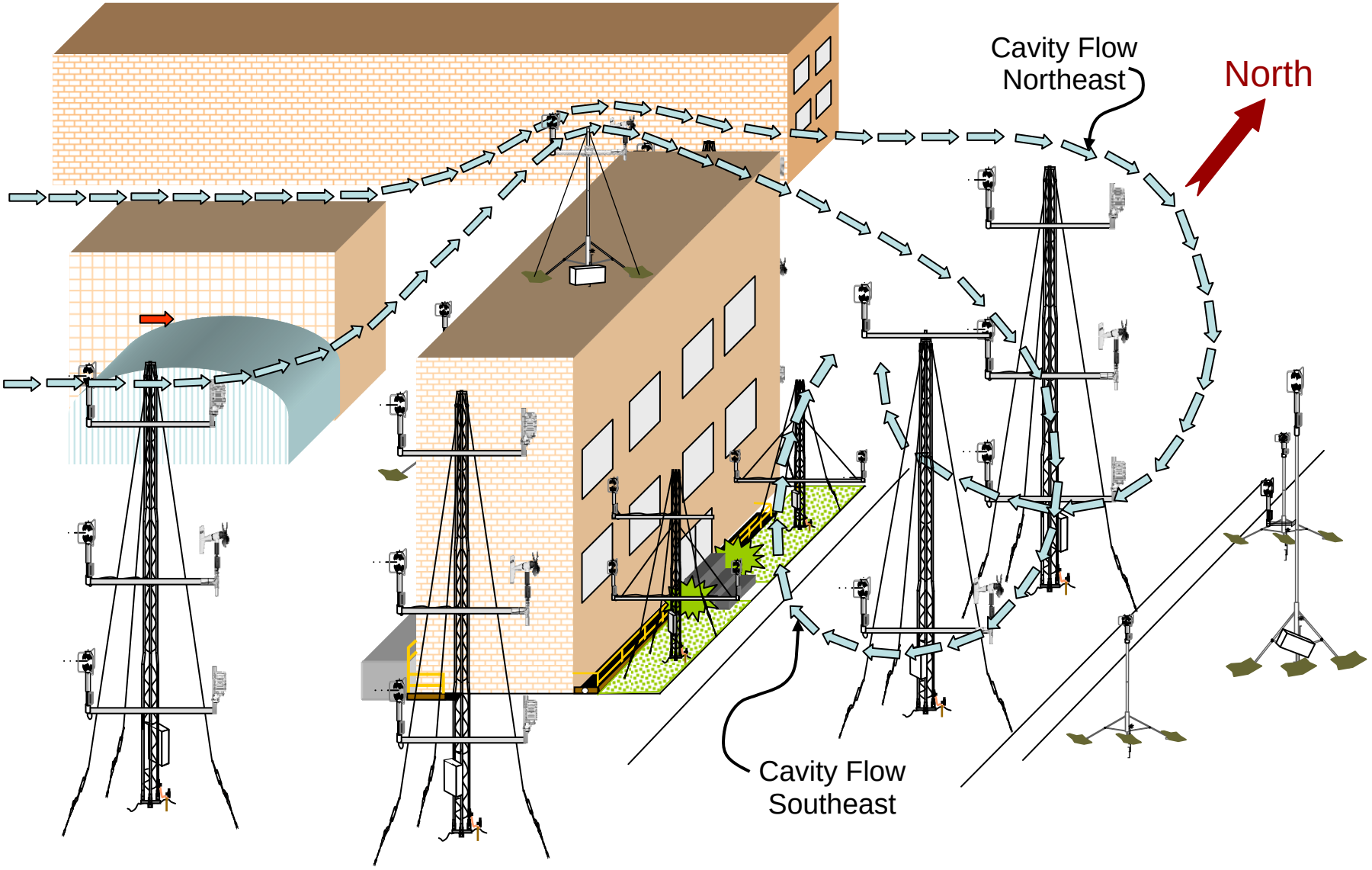

Figure A-5. Schematic of the *W07US* building leeside "flow reversal" or Cavity Flow features around the Northeast and Southeast towers.

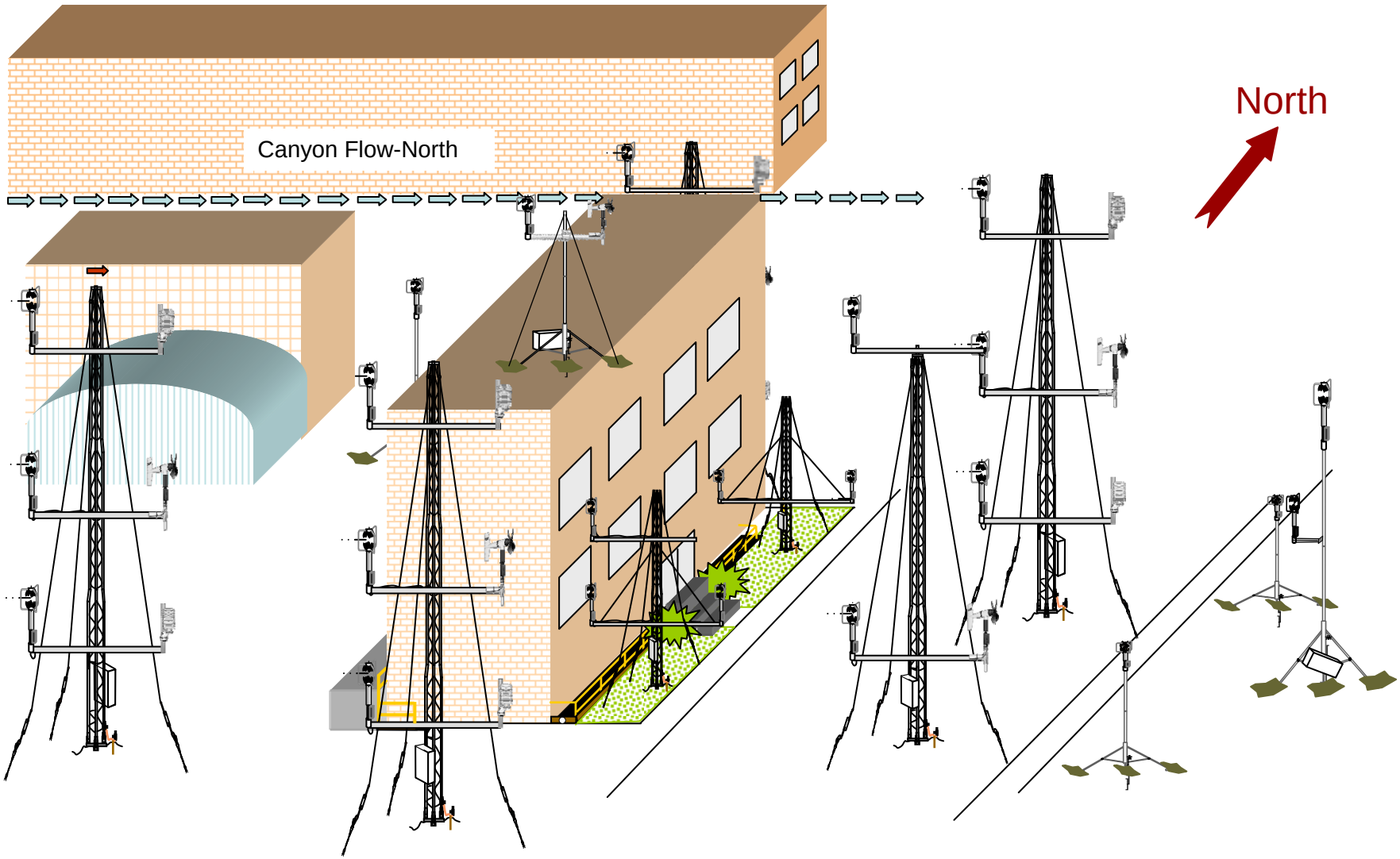

Not to Scale

Figure A-6. Schematic of the *W07US* Canyon Flow-North.

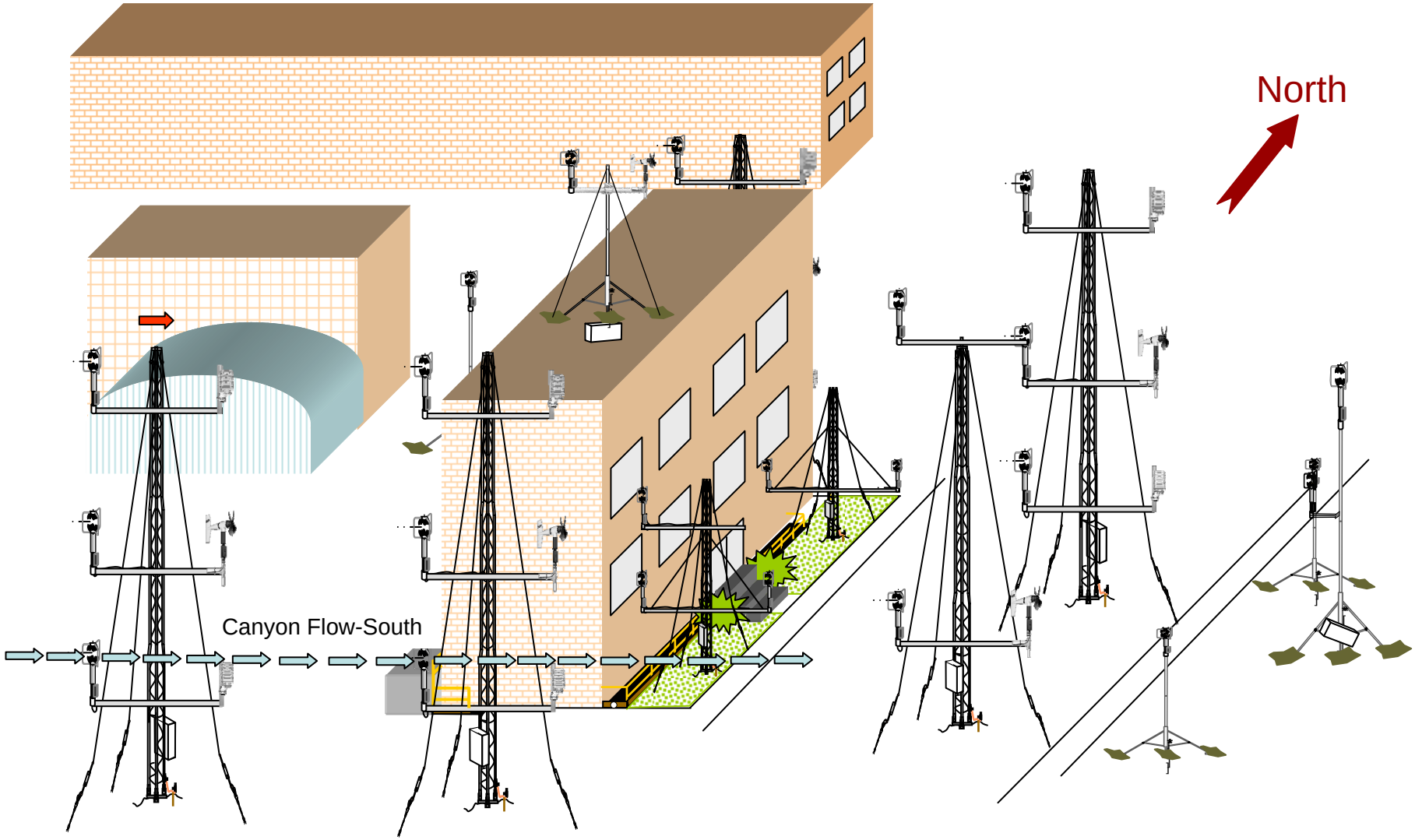

Not to Scale

Figure A-7. Schematic of the *W07US* Canyon Flow-South.

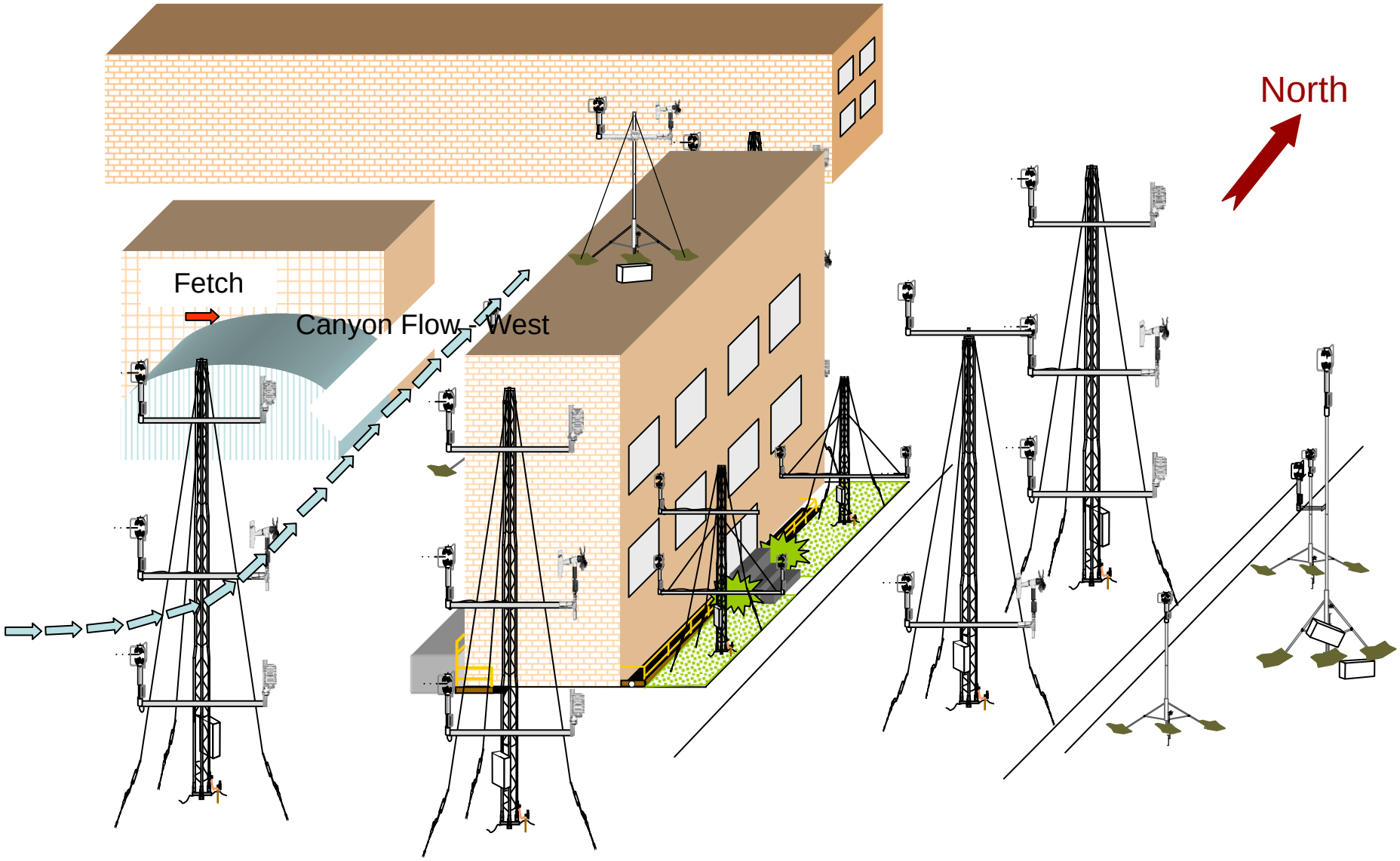

Figure A-8. Schematic of the *W07US* Canyon Flow-West.

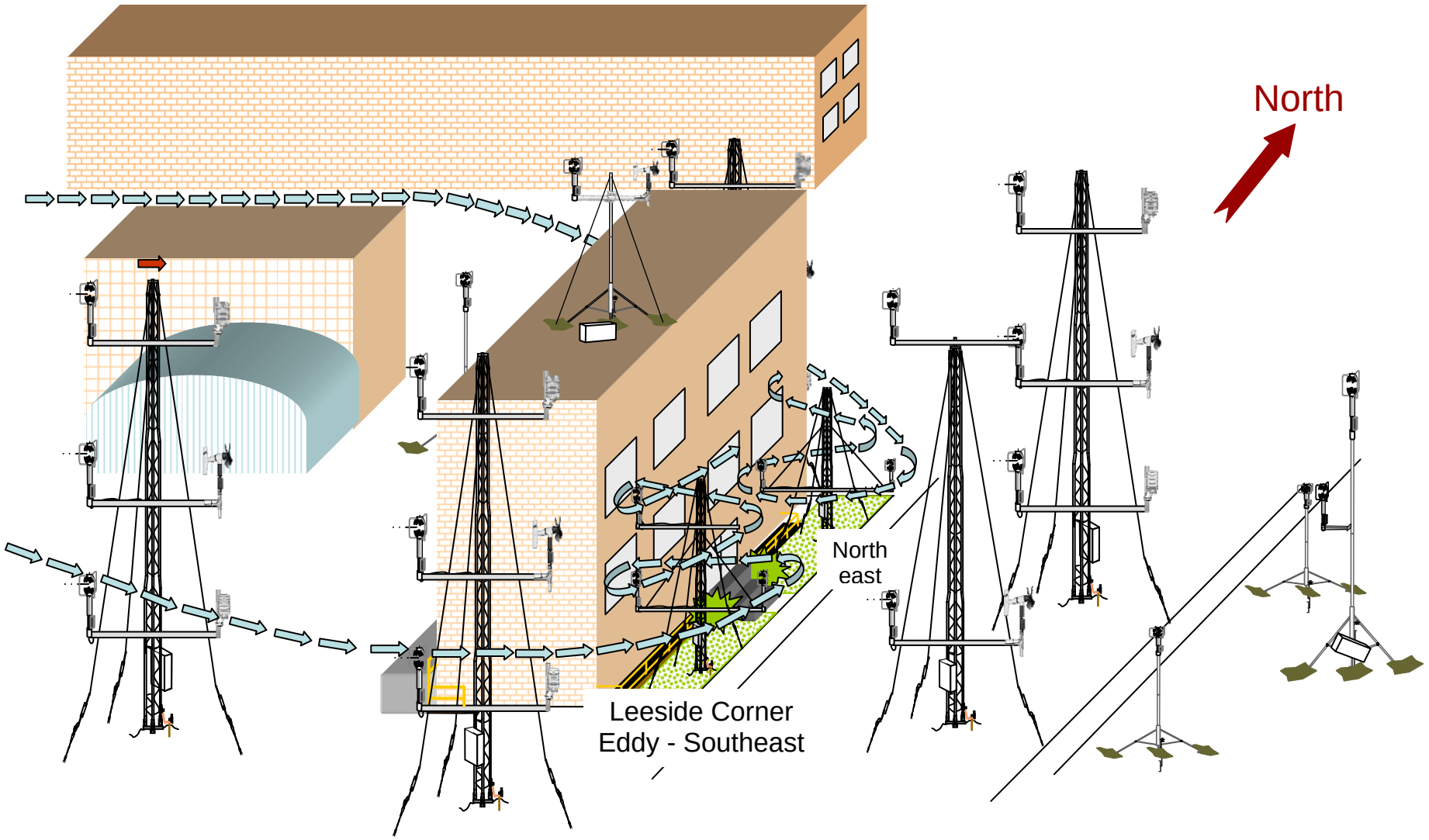

Not to Scale

Figure A-9. Schematic of the *W07US* Leeside Corner Eddies or vortices, located on the northeast and southeast corners of the subject building.

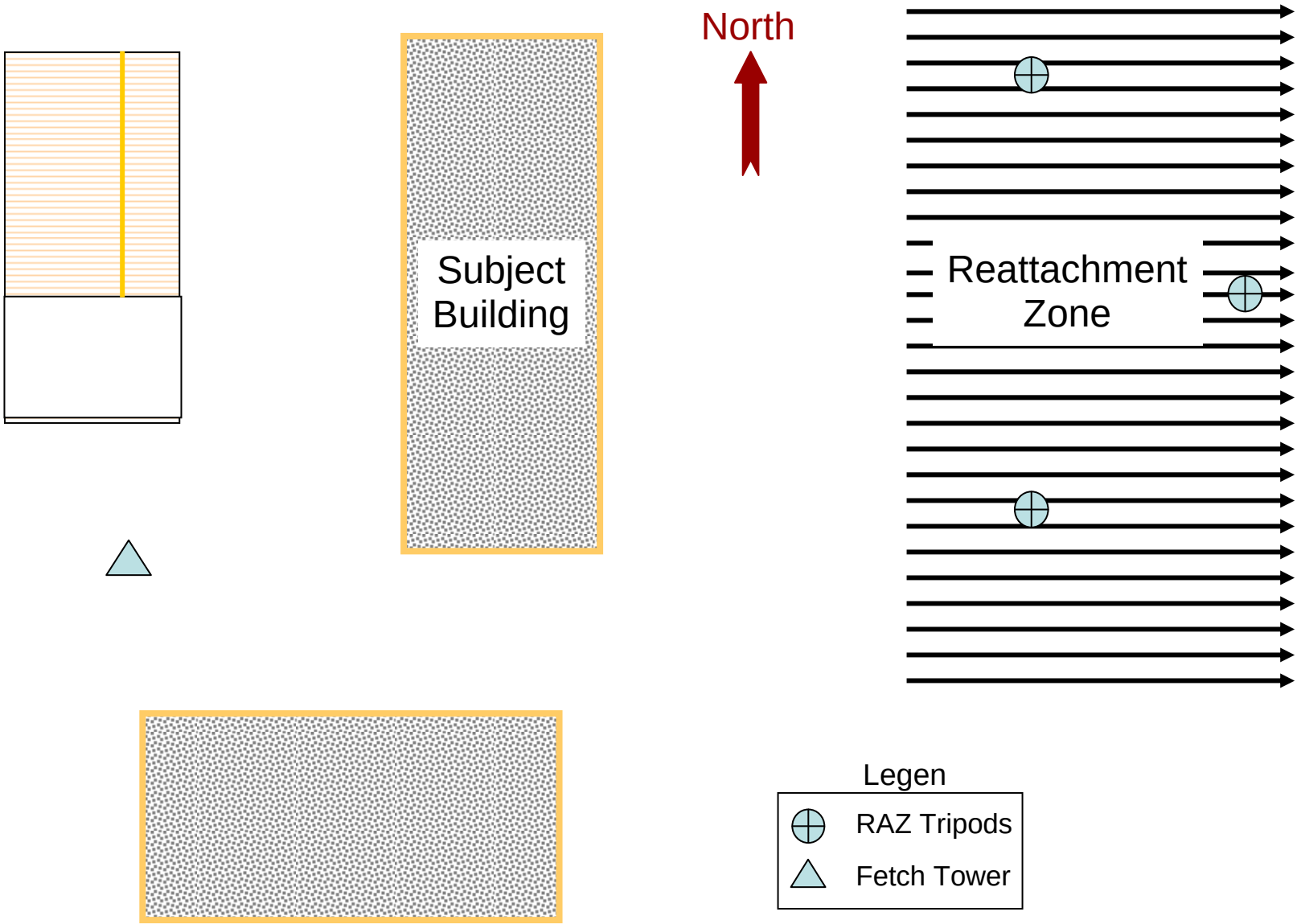

Figure A-10. Schematic of the *W07US* leeside RAZ; the long black arrows show the idealized westerly flow in the RAZ.

INTENTIONALLY LEFT BLANK.

Appendix B. Airflow Feature Time Series

The statistical results presented in this report were based on extracting just the "idealized" airflow feature. Additional insights into the airflow feature's character can be gained by examining the wind speed and wind direction time series coincident with the feature's occurrence. Table B-1 lists the location for each *W07US* airflow feature time series example within this technical report.

Table B-1. *W07US* airflow feature time series examples and their location within this technical report.

Airflow Feature	Time Series Example Within this Technical Report
Velocity Acceleration	Figure B-1
Velocity Deficit	Figure B-1
Cavity Flow-Northeast	Figure B-2
Cavity Flow-Southeast	Figure B-2
Canyon Flow-North	Figure 16
Canyon Flow-South	Figure 17
Canyon Flow-West	Figure B-3
Leeside Corner Eddies-Northeast	Figure B-4
Leeside Corner Eddies-Southeast	Figure B-4
RAZ-North	Figure 18
RAZ-East	Figure 18
RAZ-South	Figure 18

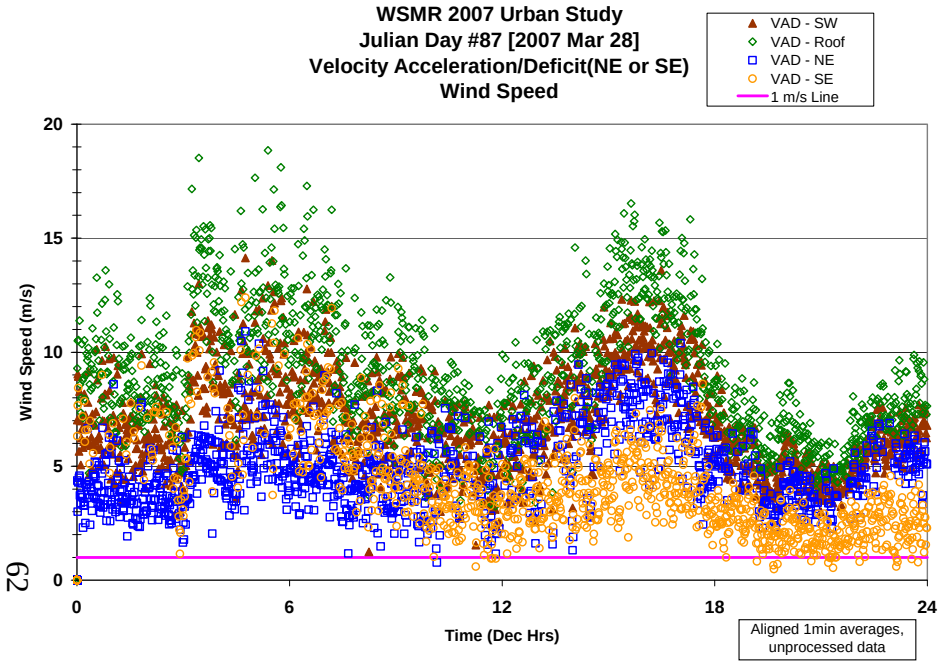

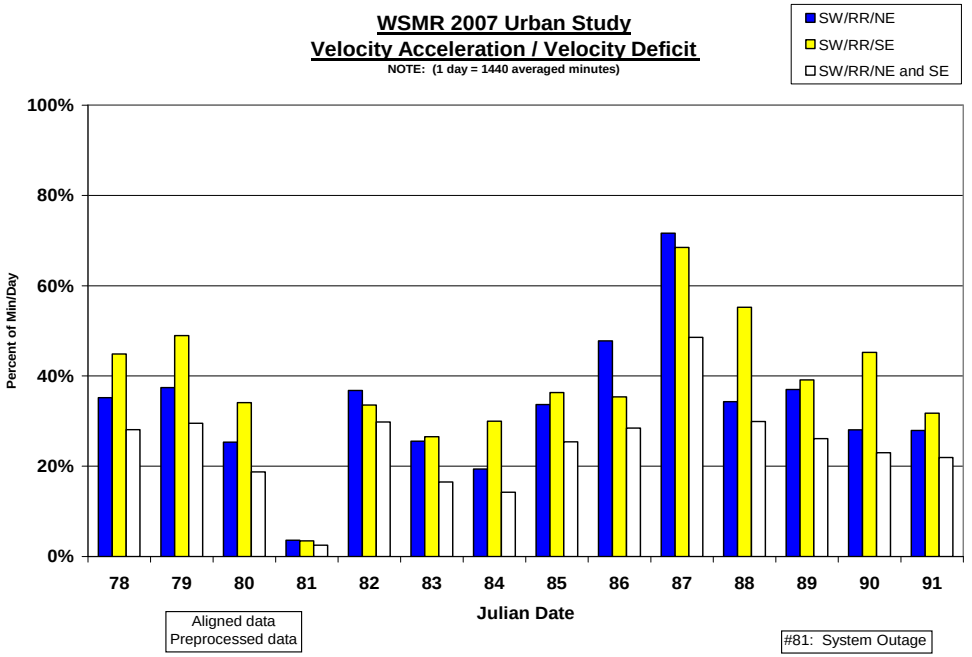

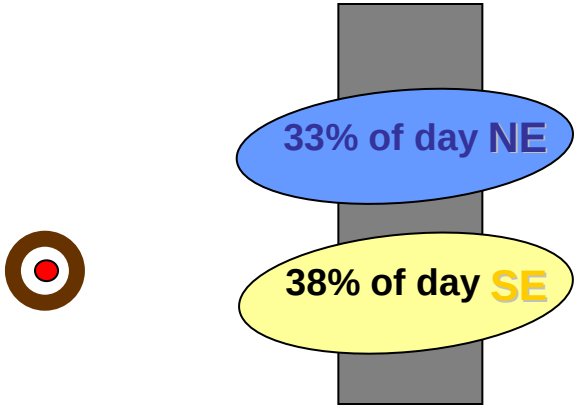

ALL DAYS
Reported
Velocity Acceleration
and
Velocity Deficit

Figure B-1. The *W07US* VAD statistical results and sample time series.

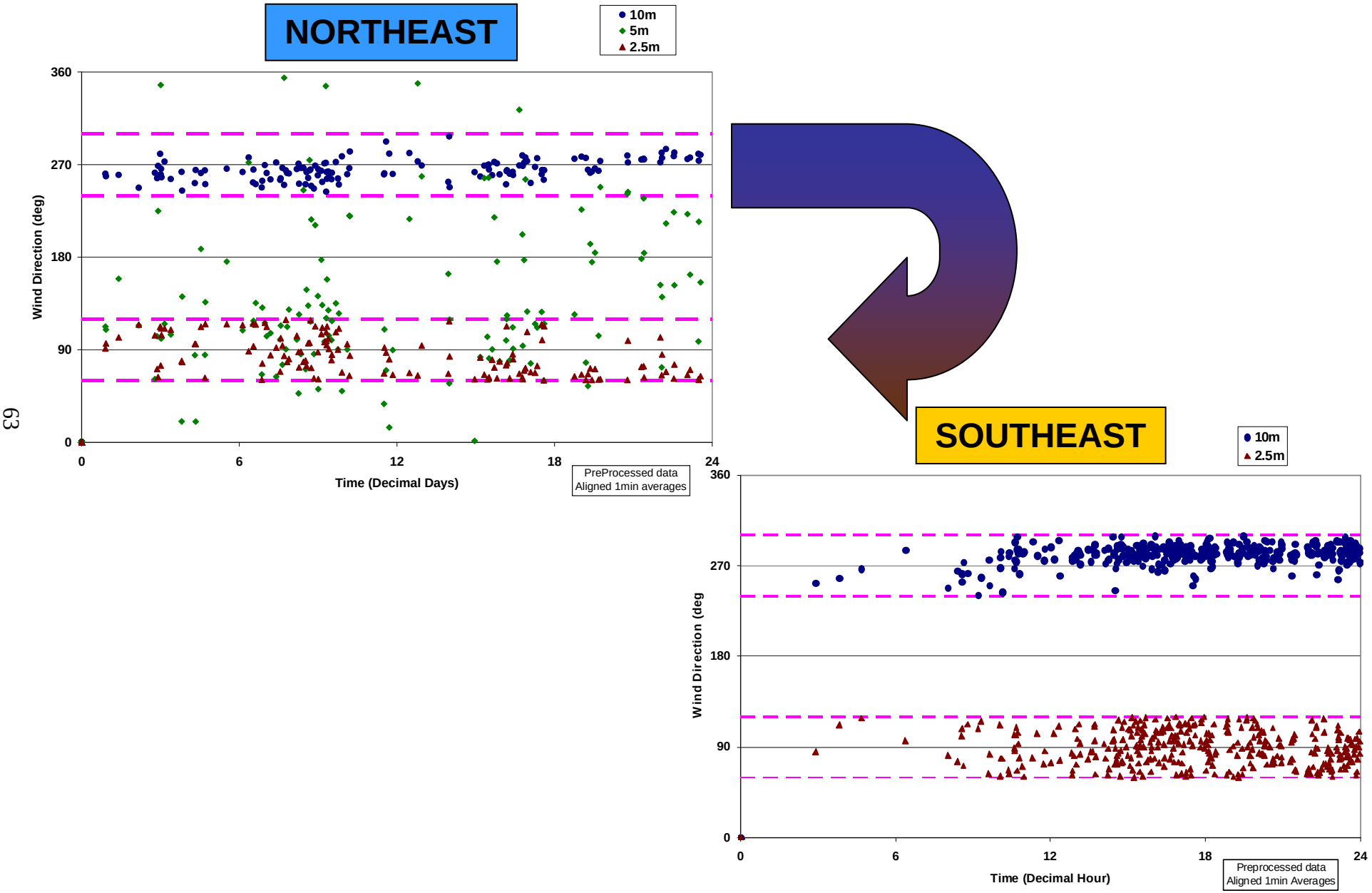

Figure B-2. The *W07US* Cavity Flow-Northeast and -Southeast statistical results and sample time series.

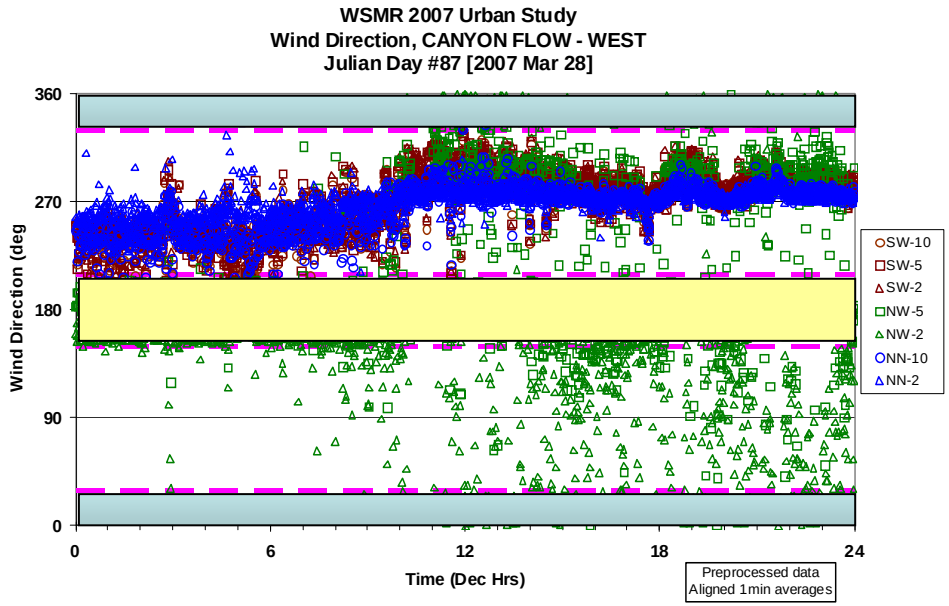

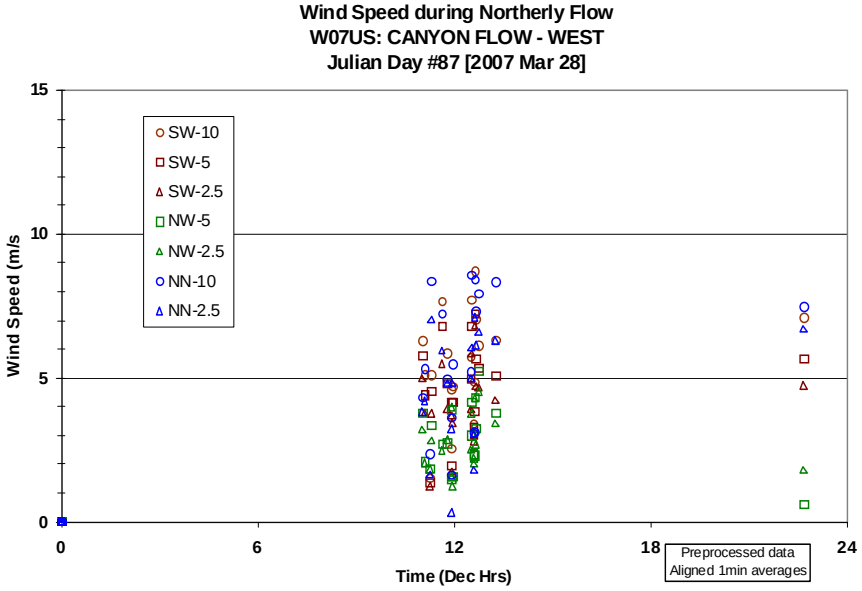

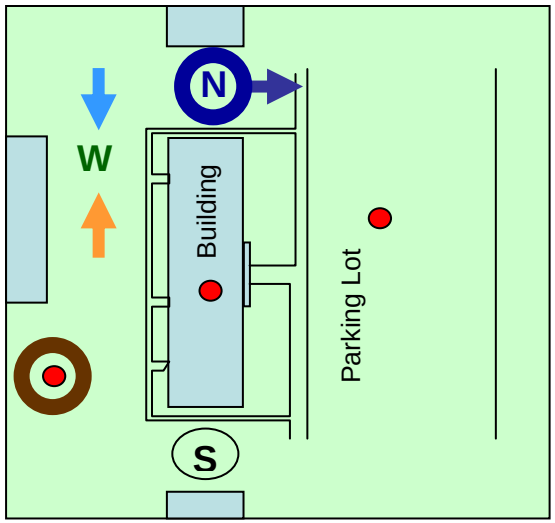

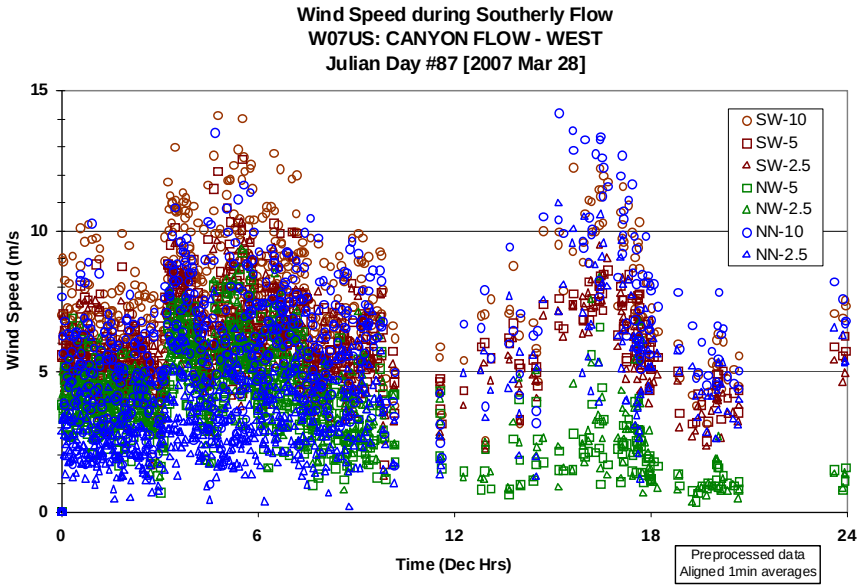

Figure B-3. The *W07US* Canyon Flow-West statistical results and sample time series.

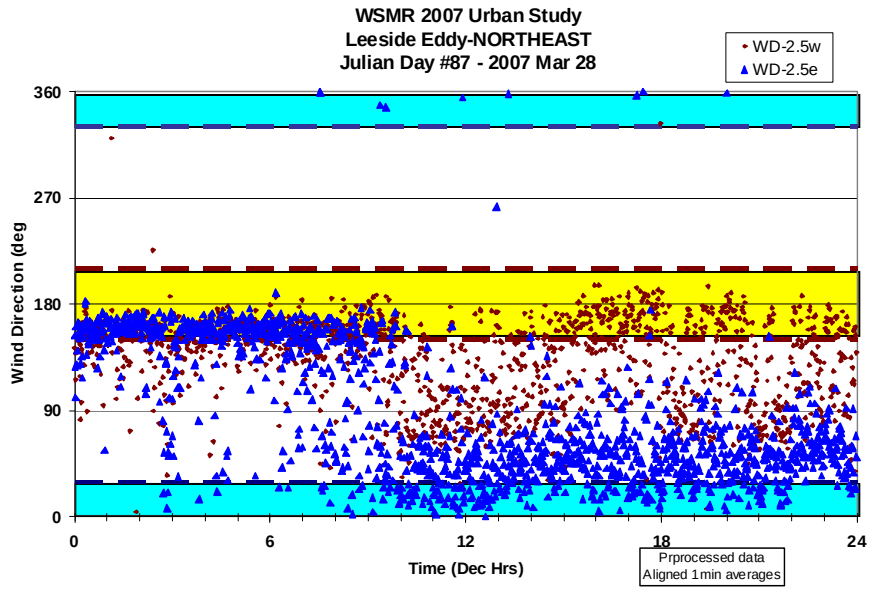

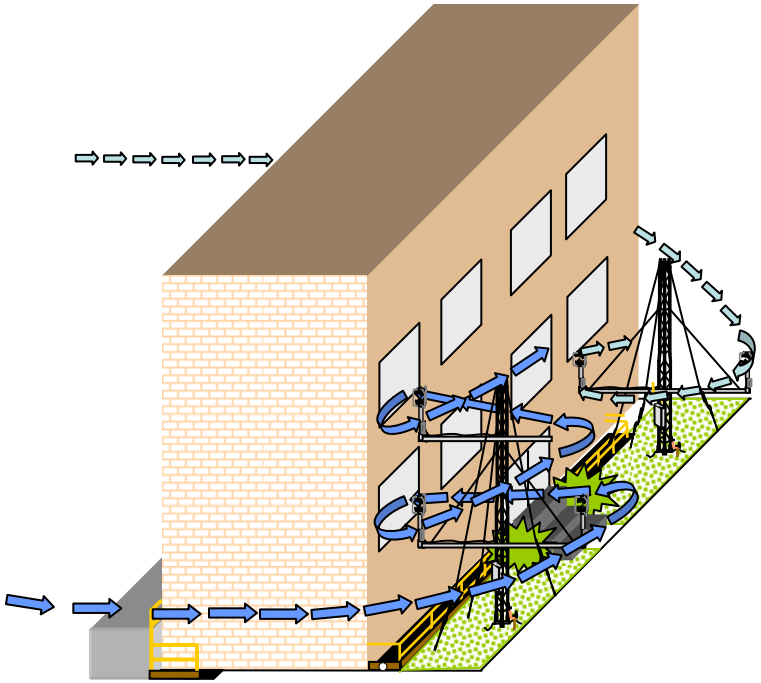

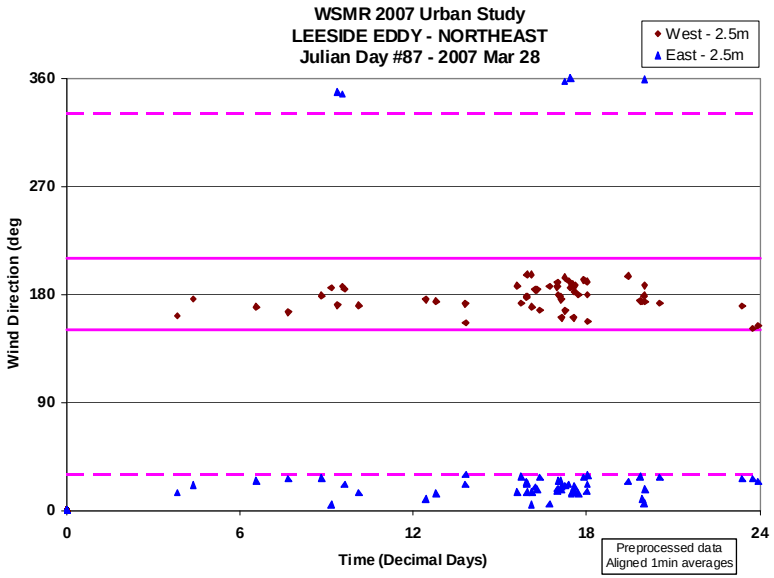

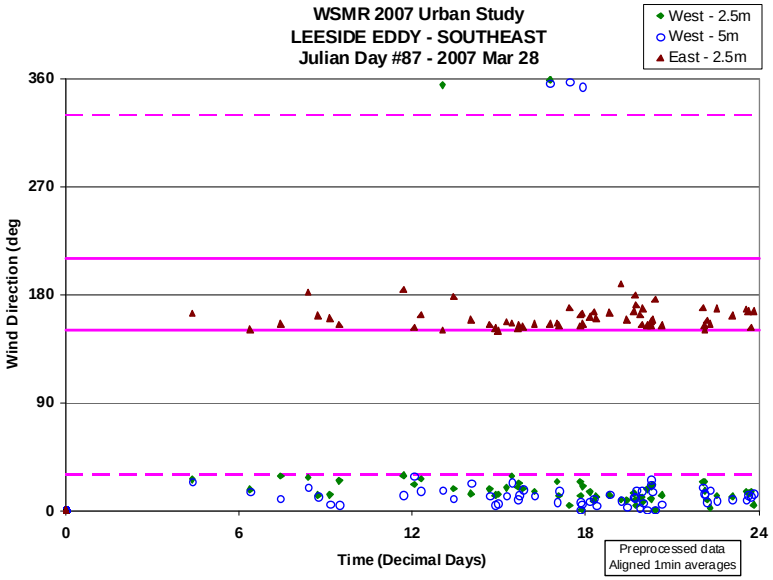

Figure B-4. The *W07US* Leeside Corner Eddy- North and -South statistical results and sample time series.

INTENTIONALLY LEFT BLANK.

Appendix C. Julian Date (JD) Versus 2007 Calendar Date

Appendix C provides a table correlating the JDs with the local *W07US* field site calendar.

Table C-1. JD versus *W07US* field site calendar.

JD	2007 Calendar Day
78	Mar 19
79	Mar 20
80	Mar 21
81	Mar 22
82	Mar 23
83	Mar 24
84	Mar 25
85	Mar 26
86	Mar 27
87	Mar 28
88	Mar 29
89	Mar 30
90	Mar 31
91	Apr 01

INTENTIONALLY LEFT BLANK.

Acronyms

3DWF	Three-Dimensional Wind Field (model)
AGL	above ground level
ARL	U.S. Army Research Laboratory
DAS	Data Acquisition System
E	east
EPA	Environmental Protection Agency
GB	gigabytes
JD	Julian Date
LANL	Los Alamos National Laboratory
LT	local time (mountain time)
N	north
NE	northeast
NOAA	National Oceanic and Atmospheric Administration
NW	northwest
NWC	northwest canyon
QUIC	Quick Urban and Industrial Complex (model)
RAZ	Reattachment Zone
RE	reattachment-east
rpm	rotations per minute
S	south
SE	southeast
VAD	Velocity Acceleration and Deficit
W	west
W03US	WSMR 2003 Urban Study

W05US	WSMR 2005 Urban Study
W07US	WSMR 2007 Urban Study
WS	wind speed
WSMR	White Sands Missile Range

No. of Copies	Organization
1 (PDF (ONLY)	ADMNSTR DEFNS TECHL INFO CTR DTIC OCP (ELECTRONIC COPY) 8725 JOHN J KINGMAN RD STE 0944 FT BELVOIR VA 22060-6218
3 CDs	US ARMY RSRCH LAB IMNE ALC IMS MAIL & RECORDS MGMT AMSRD ARL CI OK TL TECHL LIB AMSRD ARL CI OK T TECHL PUB 2800 POWDER MILL ROAD ADELPHI MD 20783-1197
1 CD	US ARMY RESEARCH LAB AMSRD CI OK TP TECHL LIB ATTN T LANDFRIED APG MD 21005
3 HCs	US ARMY RSRCH LAB AMSRD ARL CI ED M BUSTILLOS S D'ARCY R BRICE WSMR NM 88002
9 HCs 6 CDs	US ARMY RSRCH LAB AMSRD ARL CI ED G VAUCHER WSMR NM 88002
Total:	(1 PDF, 12 HCs, 10 CDs)

INTENTIONALLY LEFT BLANK.